

Copyright Warning & Restrictions

The copyright law of the United States (Title 17, United States Code) governs the making of photocopies or other reproductions of copyrighted material.

Under certain conditions specified in the law, libraries and archives are authorized to furnish a photocopy or other reproduction. One of these specified conditions is that the photocopy or reproduction is not to be “used for any purpose other than private study, scholarship, or research.” If a user makes a request for, or later uses, a photocopy or reproduction for purposes in excess of “fair use” that user may be liable for copyright infringement,

This institution reserves the right to refuse to accept a copying order if, in its judgment, fulfillment of the order would involve violation of copyright law.

Please Note: The author retains the copyright while the New Jersey Institute of Technology reserves the right to distribute this thesis or dissertation

Printing note: If you do not wish to print this page, then select “Pages from: first page # to: last page #” on the print dialog screen

The Van Houten library has removed some of the personal information and all signatures from the approval page and biographical sketches of theses and dissertations in order to protect the identity of NJIT graduates and faculty.

ABSTRACT

Title of Thesis : Reactions of Atomic Hydrogen with Chloroform
in a Discharge Flow Reactor

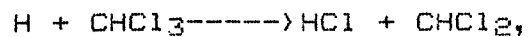
Wan-kuen Jo, Master of Science in Chemistry, 1985

Thesis Directed by : Dr. Joseph W. Bozzelli,
Professor in Department of
Chemical Engineering and Chemistry

The reactions of atomic hydrogen with chloroform were studied in a tubular flow reactor both in a 4 cm i.d. and 2.6 i.d. discharge flow reactor at pressure of 2.22 to 2.82 mmHg and room temperature using GC and GC/MS for analysis of the reaction. The hydrogen atom concentration at the reaction flame was measured by Chemiluminescence titration with nitrogen dioxide. The hydrogen concentrations are in the 2.48×10^{14} to 4.83×10^{14} atoms/cc range at six different hydrogen flow rates. Evidence was found for the formation of atomic carbon intermediate in the reaction, but methane was the primary final product in both reactions for reaction times of 0.024 sec to 0.072 sec.

We propose a mechanism for the secondary reactions that almost all chloroform consumed went toward the production of methane. Thermochemical data were calculated for this purpose and energy studies were done along with analysis of many references. The Kinetics were computer-simulated by solving the simultaneous first-order differential equations describing the time dependence of the concentrations of the various chemical species, using both Runge-Kutta method for integration and Rosenbrock method for optimization of the system. Through this

computer modelling of a reaction scheme and comparison with experimental data the rate constants for the primary reaction of hydrogen atom with chloroform at 298 K,



was determined to be 4.2×10^{-14} cc/molecule sec. This value was larger than that determined in the only earlier study unpublished (23).

REACTION OF ATOMIC HYDROGEN WITH CHLOROFORM
IN A DISCHARGE FLOW REACTOR

Wan - Kuen by Jo

Thesis submitted to the Faculty of the Graduate School of
the New Jersey Institute of Technology in partial fulfillment of
the requirements for the degree of
Master of Science
1985

APPROVAL SHEET

Title of Thesis : Reaction of Atomic Hydrogen with Chloroform
in a Discharge Flow Reactor

Name of Candidate : Wan - kuen Jo
Master of Science, 1985

Thesis and Abstract Approved :

~~_____~~
Dr. Joseph W. Ezzelli
Professor Department
of Chemical Engineering
and Chemistry

May 7, 1985

Date

May 7, 1985

Date

May 7, 1985

Date

VITA

Name : Wan-kuen Jo

Permanent address :

Degree and date to be conferred : Master of Science, 1985

Date of birth :

Secondary education : Masan High School February 20, 1975

Collegiate institutions attended	Date	Degree	Date of Degree
Kyung-pook National University	3/75-2/82	B.S.	2/82
Army of Korea	10/77-5/80		
New Jersey Institute of Technology	1/83-5/85		5/85

Major : Chemistry

ACKNOWLEDGEMENTS

It is my pleasant duty to express my sincere thanks to Dr. Joseph W Bozzelli for his guidance, kindness and encouragement.

TABLE OF CONTENTS

1.	INTRODUCTION -----	1
2.	THEORY -----	4
	A. REACTION -----	4
	B. GAS CHROMATOGRAPHY -----	5
	C. HYDROGEN ATOM TITRATION -----	6
	D. CHEMICAL KINETICS -----	11
	i. THERMOCHEMISTRY -----	11
	ii. KINETICS -----	12
3.	EXPERIMENTAL APPARATUS AND PROCEDURES -----	17
4.	RESULTS AND DISCUSSION -----	34
	A. EXPERIMENTAL RESULTS -----	34
	B. HYDROGEN ATOM CONCENTRATIONS -----	38
	C. REACTION MECHANISM -----	43
	D. COMPUTER MODELLING AND DISCUSSION -----	47
5.	CONCLUSIONS -----	59
	APPENDIX -----	62
	i. NO ₂ AND N ₂ O ₄ FRACTION -----	62
	ii. ESTIMATION OF RATE CONSTANT BY BENSON'S METHOD -----	64
	iii. REACTIONS -----	65
	iv. CALCULATION OF HYDROGEN ATOM AND CHLOROFORM CONCENTRATIONS -----	66
	v. COMPUTER MODEL -----	68
	REFERENCES -----	78

Table of Figures

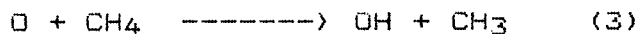
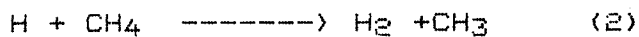
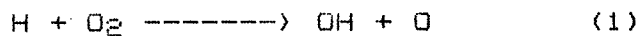
Figure 1	-----	Fractions of NO ₂ , N ₂ O ₄ , Ar to change of total pressure in cylinder. -----	10
Figure 2	-----	Constrained Rosenbrock (Hill Algorithm) Logic. -----	16
Figure 3	-----	Experimental Setup. -----	18
Figure 4	-----	Schematic Diagram of the 4-port Hamiltonian Injection Valve. -----	24
Figure 5	-----	Schematic Diagram of the 6-port Hamiltonian Injection Valve. -----	25
Figure 6	-----	Operation of the 4-port Hamiltonian Injection Valve. -----	27
Figure 7	-----	Operation of the 6-port Hamiltonian Injection Valve. -----	28
Figure 8	-----	H-CHCl ₃ Experimental Curves at five different H ₂ flow rate. -----	36
Figure 9	-----	H-CHCl ₃ Experimental Curves at two different reaction time. -----	37
Figure 10	-----	Hydrogen Atom Titration Curves with NO ₂ at three different H ₂ flow rate. -----	39
Figure 11	-----	Hydrogen Atom Titration Curves with NO ₂ at two different H ₂ flow rate. -----	40
Figure 12	-----	Hydrogen Atom Titration Curves with NO ₂ at a H ₂ flow rate. -----	41
Figure 13	-----	H-CHCl ₃ Experimental and Computer Model Curves at 0.14 cc/sec (H ₂). -----	49
Figure 14	-----	H-CHCl ₃ Experimental and Computer Model Curves at 0.4 cc/sec (H ₂). -----	50
Figure 15	-----	H-CHCl ₃ Experimental and Computer Model Curves at 0.62 cc/sec (H ₂). -----	51
Figure 16	-----	H-CHCl ₃ Experimental and Computer Model Curves at 0.82 cc/sec (H ₂). -----	52
Figure 17	-----	H-CHCl ₃ Experimental and Computer Model Curves at 1.1 cc/sec (H ₂). -----	53
Figure 18	-----	H-CHCl ₃ Experimental and Computer Model Curves at 0.028 sec (Reaction Time)--	54

Figure 19 ----- H-CHCl3 Experimental and Computer Model
Curves at 0.072 sec (Reaction Time)-55

1. INTRODUCTION

Halogen substituted methanes, such as CHCl_3 , have been found to be a rather strong flame inhibitor (1-3), especially for hydrocarbon-oxygen flames (4). However, the mechanisms and the kinetics of this inhibition have not been fully determined.

It is the purpose of this research to study the chemical kinetics and product formation of the reaction of atomic hydrogen with chloroform. This reaction and its subsequent reactions are suspected to account for the flame inhibition because of the removal of H atoms from the flame propagation step. The removal of the atomic hydrogen, resulting from the reaction of hydrogen atoms with chloroform, inhibits the chain branching reaction with oxygen (eqn.1), a chain reaction with fuel (eqn.2), and a chain reaction of O with fuel (eqn.3).



Furthermore, CH_3 radical would rapidly undergo oxidative reactions, which are important in fuel-rich flames (5,6). It is, therefore, postulated that small amounts of inhibitors (halomethanes) compete for hydrogen atoms with large amounts of O_2 ; the activation energy of the inhibition reactions is low while that of the above chain-branching reactions is relatively high (6,7).

Many halomethanes are known or suspected to be carcinogenic and the principal products of inhibition reactions where no

oxygen is present or very low O_2 levels exist are methane and an acid, such as HCl, as found in this study. It is possible, therefore, that inhibition reactions could lead to a method for the destruction (conversion) of toxic wastes such as PCB, chlorinated pesticide, with the simultaneous production of a fuel and a recycle of HCl.

There has not been much work done in the past several decades on the study and mechanism of the reaction of atomic hydrogen with halomethanes. Gaydon and Wolfhard (8) were the first to report flame-like emission from atomic hydrogen reactions with several halocarbons. In addition, they characterized the emitting species as mostly C_2 and CH. M. Costes et al. (9) have recently used reactions of hydrogen with halocarbons to produce atomic carbon for studies of the chemistry of this species. Arnold, Kimbell, and Snelling (10) have observed C_2 visible and infrared emissions in the reactions of atomic hydrogen with halomethanes, but neither hydrogen atom concentrations, stoichiometry, nor stable end products were monitored. Observing the various emissions from a fast reaction could yield a wealth of information about various intermediates, even if they are of very short lifetimes. For instance, if a CH emission is observed in a flame, the CH radical in an excited state is being formed somewhere in the reaction scheme. Any representative model would have to incorporate such a step.

The stoichiometric analysis of end products was not done in any of the previous studies, except in the work by Jones et al. (11), where he found accurate measurement of the hydrogen

atom concentration was a problem. The kinetics on the reaction of atomic hydrogen with chloroform have only scarcely been studied. Furthermore, there is no rate-constant available for the reaction. Gould et.al.(12) have recently studied the reaction of hydrogen atoms generated by photolysis of HBr or HI with $CDCl_3$. Gould et.al.(12) obtained the ratio of the integral probabilities of Cl abstraction and of D abstraction, when normalized to equal numbers of Cl and D atoms; but, not rate constant for the reaction. Considering H + halomethane reactions in flame inhibition, possible conversion of toxic waste into fuels, and the study of atomic hydrogen reactions in general, it was strongly felt that a through investigation into the kinetics and mechanism of the reactions of atomic hydrogen with chloroform should be undertaken. Through UV-visible Chemiluminescence from the reaction flame, combined with gas chromatographic analysis of the stable end products, interferences were made. Then a possible mechanism was postulated and the kinetics simulated on an Univac 90/80-3 computer. It was solved the simultaneous first-order differential equations describing the time dependence of the concentrations of the various chemical species by both Runge-Kutta Forth Integration Method(13) and a Rosenbrock optimization Method(14).

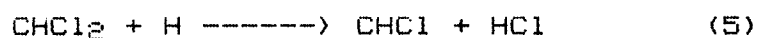
II. THEORY

A. Reaction

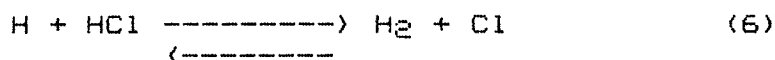
The reaction of hydrogen atoms with chloroform, involving abstraction of an Cl atom, and leading to formation of HCl, constitutes the first step in a large series of elementary reactions. Therefore, the major factor that complicates the study of the reactions of atomic hydrogen with halomethanes stems not from the primary reaction, but from the multitude of rapid secondary reactions that follow. The primary reaction, for example, with chloroform:



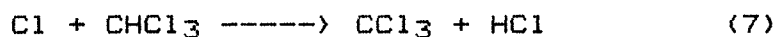
leads to the formation of CH_2Cl , an extremely reactive molecule because of its unpaired electron. Consequently, it reacts almost immediately with atomic hydrogen to form other reactive species as, for instance, CHCl (eqn. 5).



Atomic chlorine is rapidly formed by the equilibrium reaction:



This reaction is also very reactive, and adds to the complexity by reacting with the primary reactant:



This reaction increases the consumption of chloroform.

These examples show how the various secondary reactions render impossible the isolation of the products of the primary reaction and necessitate the studying of the many reactions as a whole, "Global Reaction System". It is essential, therefore,

that the reaction model incorporate all the important secondary reactions in order to be a plausible representation.

The reactions are studied in a 1.0 - 1.1 meter long tubular flow reactor, with atomic hydrogen introduced at the top of the tube, and the halomethane let in through a movable Teflon injector tube. The resulting reaction flame is analysed both chromatographically and spectroscopically.

B. Gas Chromatography

Gas-liquid Chromatography (GLC) accomplishes a separation by partitioning solutes between a mobile gas phase and a stationary liquid phase held on a solid support.

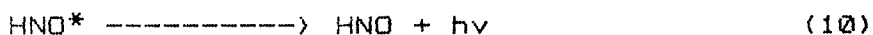
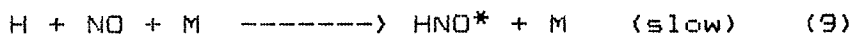
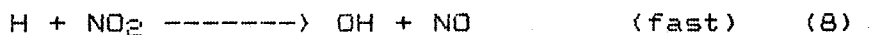
The sequence of a gas chromatographic separation is as follows. A sample containing the vapors in our system is swept as a flow of vapor by the carrier gas stream into the column inlet via a heated inlet line. The solutes are adsorbed at the head of the column by the stationary phase and then desorbed by fresh carrier gas. The sorption-desorption process occurs repeatedly as the sample is moved toward the column outlet by the carrier (mobile phase) gas. Each solute will travel at its own rate through the column. Each solute will separate to a degree determined by the individual partition ratios and the extent of band spreading. The solutes are eluted sequentially in the increasing order of their partition ratios and enter a detector attached to the column exit. A recorder is used and the signals appear on the chart as a plot of time versus the composition of the carrier gas stream. The time of emergencies of a peak is

characteristic for each component: the peak area is proportional to the concentration of the component in the mixture.

A gas chromatograph in this study consists of six parts: (1), a supply of carrier gas in a high pressure regulators and flow meters, and a valve to introduce extra make-up gas to some detectors, (2) a sample injection system, (3) the detector, (5) an electrometer, strip-chart recorder and integrator, and (6) separate thermostated compartments for housing the column and the detector so as to regulate their temperature, or to program the column temperature.

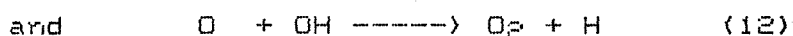
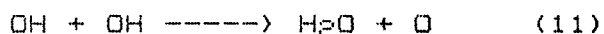
(C) Hydrogen Atom Titration

Hydrogen atom concentrations are determined in flow discharge systems by allowing NO_2 to take the path normally taken by the halomethane, and a reaction flame resulted. The reaction flame is also in the visible spectral range--it could be seen--and it is whitish in color because of the combined effect of the various emissions. The radiating species in this case, HNO, emits primarily in the wavelength range of 686.5-698.5nm (15). The intensity of the HNO emission could now be monitored by setting the spectrometer at 692.8nm. The various reactions occurring are



where * denotes an excited molecule, and M is either another molecule or the wall, which remove some of HNO*'s excess energy,

so it does not immediately dissociate. There is a fixed amount of hydrogen atoms present in the reaction, so if enough NO_2 is supplied to react with all H's, there should be no more H left over for reaction(8). At this point the emission would be just eliminated, there being no HNO^* produced. The NO_2 flow is, therefore, increased to the point where the flame just disappears after its peak intensity, as indicated by a minimum in the current to the picoammeter from the PMT. Since NO_2 and H are in stoichiometric quantities at this point, the H atom concentration may be readily calculated from the NO_2 flow rate. In practice, however, the H atom concentration may actually be larger than the NO_2 used (16) owing to the fast reactions of:



This ratio also depends on the type of reactor, coating used on the walls, and reaction times.

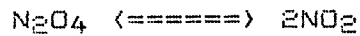
It must be mentioned that the NO_2 used here came from a cylinder that was flushed several times with argon, evacuated to 0.025 atm, then filled to the extent of 0.357 atm with NO_2 , and the pressurized to 2.065 atm with argon. At a partial pressure of 0.332 atm (252 mmHg), NO_2 exists in equilibrium with N_2O_4 , and in fact, it is equilibrium compositions that pass through the rotameter. It must be considered here that as the pressure in the cylinder decreases, the actual fraction of NO_2 and N_2O_4 changes with the total pressure change. In this study, equilibrium constant, K_p , of NO_2 - N_2O_4 system (17) is 0.1134 atm and partial pressure of NO_2 and N_2O_4 in the cylinder is

calculated as follows at two different total pressure:

(i) first, at total pressure, 1550.5 mmHg (Ar + NO₂ + N₂O₄)

$$p(\text{NO}_2 + \text{N}_2\text{O}_4) = \frac{252 \text{ mmHg}}{760} = 0.3316 \text{ atm}$$

for the system,



$$K_P = \frac{(P(\text{NO}_2))^2}{P(\text{N}_2\text{O}_4)} = \frac{(P(\text{NO}_2))^2}{P(\text{NO}_2 + \text{N}_2\text{O}_4) - P(\text{NO}_2)}$$

$$= 0.1134 \text{ atm.}$$

Solving above equation for P(NO₂), P(NO₂) = 0.1453 (atm) = 110.43

(mmHg) and P(N₂O₄) = P(NO₂ + N₂O₄) - P(NO₂) =

$$0.3316 - 0.1453 = 0.1863 \text{ (atm)} = 141.57 \text{ (mmHg)}.$$

Therefore, the fraction of P(NO₂+N₂O₄) to the total pressure,

$$F(\text{NO}_2 + \text{N}_2\text{O}_4) = \frac{252}{1550.5} = 0.1625$$

$$\text{and } F(\text{Ar}) = 1.0 - 0.1625 = 0.8375$$

(ii) Next, at total pressure, 1450.5 mmHg

$$P(\text{NO}_2) = 0.1392 \text{ (atm)} = 105.792 \text{ (mmHg)} \quad \text{and } P(\text{N}_2\text{O}_4) = P(\text{NO}_2 + \text{N}_2\text{O}_4)$$

$$- P(\text{NO}_2) = 0.3102 - 0.1392 = 0.171 \text{ (atm)} = 129.958 \text{ (mmHg)}$$

Assuming that fraction of NO₂ + N₂O₄ to that of argon at 1550.5 mmHg is still same as that at 1450.5 mmHg, the above calculation is correct. In practice as total pressure decreases the actual fraction of NO₂ + N₂O₄ to that of argon increases somewhat because the ratio of N₂O₄ to NO₂ becomes larger at lower total pressure and more N₂O₄ is dissociated to NO₂ resulting in the increase of the fraction of NO₂ + N₂O₄ to that of argon. This is

explained by the following calculation:

(a) At total pressure, 1550 mmHg, $P(\text{NO}_2 + \text{N}_2\text{O}_4) = 252 \text{ mmHg}$ and the fraction of N_2O_4 to that of NO_2 ,

$$F(\text{N}_2\text{O}_4) = \frac{P(\text{N}_2\text{O}_4)}{P(\text{N}_2\text{O}_4 + \text{NO}_2)} = \frac{141.57}{252} = 0.562$$

$$F(\text{NO}_2) = 1 - F(\text{N}_2\text{O}_4) = 1 - 0.562 = 0.438$$

(b) At total pressure, 1450.5 mmHg, $P(\text{NO}_2 + \text{N}_2\text{O}_4) = 235.75 \text{ mmHg}$ and the fraction of N_2O_4 to that of NO_2 ,

$$F(\text{N}_2\text{O}_4) = \frac{P(\text{N}_2\text{O}_4)}{P(\text{N}_2\text{O}_4 + \text{NO}_2)} = \frac{129.96}{235.75} = 0.551$$

$$\text{and } F(\text{NO}_2) = 1 - F(\text{N}_2\text{O}_4) = 1 - 0.551 = 0.4488.$$

Comparing (a) with (b), the difference of $F(\text{N}_2\text{O}_4)$ is:

$F(\text{N}_2\text{O}_4) = 0.562 - 0.551 = 0.011$ for the change of total pressure, 1550.5 mmHg to 1450.5 mmHg where F means fraction. Since every N_2O_4 dissociation gives 2NO_2 's, change in $F(\text{N}_2\text{O}_4)$ thus represents the fraction of volume NO_2 gained. So, increase in NO_2 is calculated as follows:

$$P(\text{NO}_2 + \text{N}_2\text{O}_4) * \text{Change in } F(\text{N}_2\text{O}_4) = 235.75 * 0.011 = 2.59 \text{ mmHg, so}$$

$$P(\text{N}_2\text{O}_4) = 129.96 \text{ mmHg, } P(\text{NO}_2) = 107.9 + 2.59 = 108.38 \text{ mmHg,}$$

$$\text{and } P(\text{NO}_2 + \text{N}_2\text{O}_4) = 235.75 + 2.59 = 238.34 \text{ mmHg}$$

Considering the change of the fraction of NO_2 and N_2O_4 to decreasing total pressure therefore, the actual $P(\text{NO}_2 + \text{N}_2\text{O}_4)$ can be obtained by the computer program at any point needed.

The mixture encounters vacuum in the halomethane manifold so here the N_2O_4 is fully converted to NO_2 and the NO_2 pressure is gotten from the figure 1 which is determined by computer program

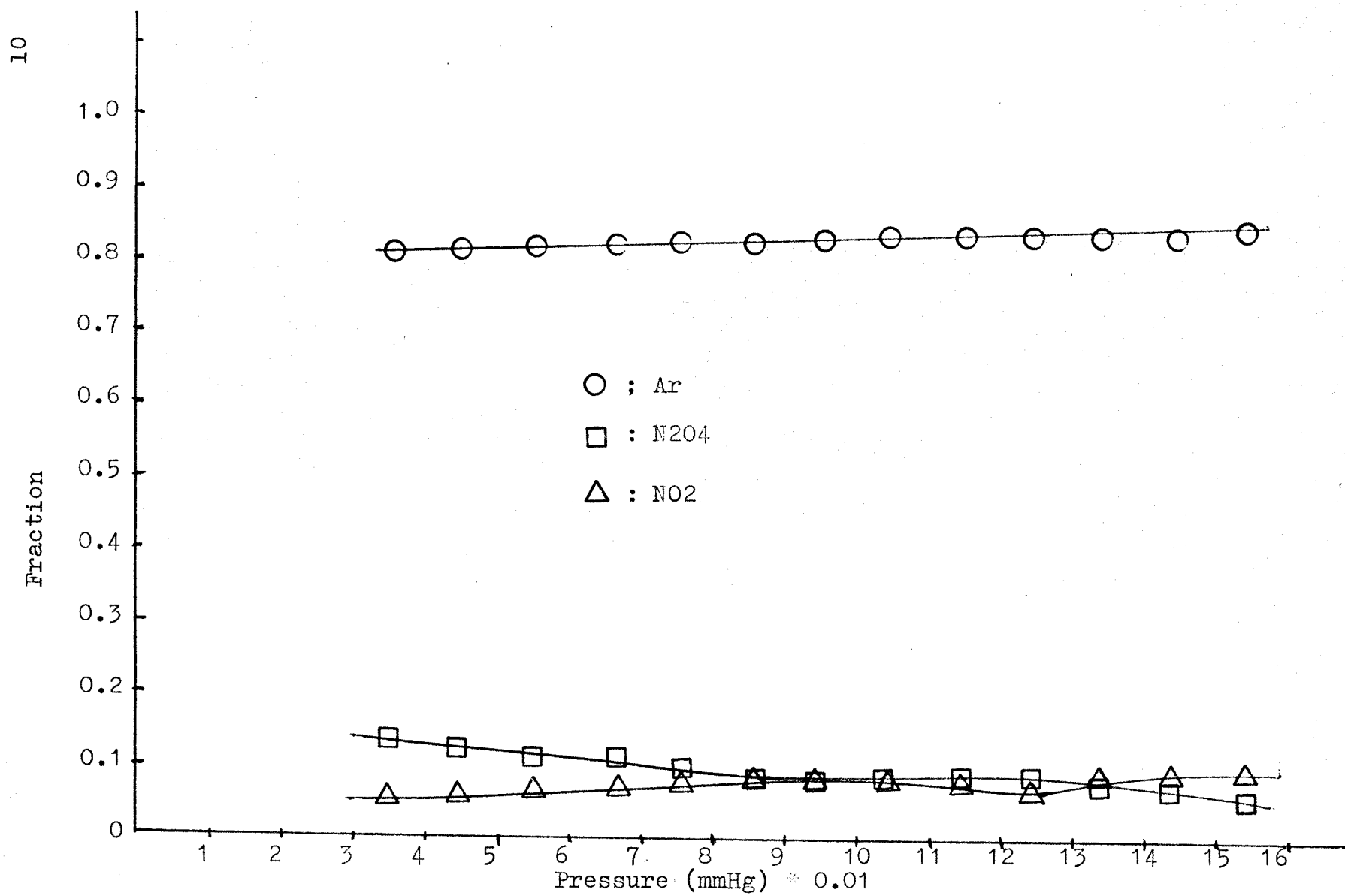


Figure 1. Fractions of NO₂, N₂O₄ and Ar to the change of total press. in cylinder.

given in appendix 1, along with some example data.

D. Chemical Kinetics

(i) Thermochemistry

Of importance to the problem of relating structure and reactivity is the thermochemistry of the reaction—that is the net enthalpy and entropy changes that occur upon the making of new bonds and the breaking of old ones. For the purpose of this study, thermo-kinetic data are approximated by Benson's additivity rules for unknown very reactive reactions. The calculations are given at appendix 2. If we consider the reaction in the following equation a large positive standard free-energy change for the reaction, ΔG^\ominus ,



means that it will not take place to any appreciable extent. On the other hand, if ΔG^\ominus is large and negative, the likelihood is that it will occur. ΔG^\ominus is a function of ΔH^\ominus and ΔS^\ominus , the standard enthalpy and entropy of reaction, respectively:

$$\Delta G^\ominus = \Delta H^\ominus - (T \cdot \Delta S^\ominus) \quad (14)$$

ΔH^\ominus is a function of the heats of formation of the molecules being formed or destroyed, and ΔS^\ominus is a function of the entropies of the molecules being formed or destroyed. Thus for the reaction in equation (13), $\Delta H^\ominus = H^\ominus_f (C) + H^\ominus_f (D) - H^\ominus_f (A) - H^\ominus_f (B)$ where $H^\ominus_f (x)$ is the standard heat of formation of x . similarly, $\Delta S^\ominus = S^\ominus (C) + S^\ominus (D) - S^\ominus (A) - S^\ominus (B)$ where $S^\ominus (x)$ is the standard entropy of x .

Experimental heats of formation are not available for all compounds, but by Benson's additivity rules ΔH^\ominus_f for this

study in the gas phase can be calculated.

(ii) Kinetics

From a chemical kinetics point of view the reaction was considered to be a plug flow reactor. Such a reactor is theoretically a steady-state flow reactor, one in which the composition at any point along the reactor is unchanged with time when inlet flows and composition are constant (18). Absolute plug flow, however, is an ideal situation, and is never attained in practice. Most "plug flow" systems try to approximate the ideal cases as closely as possible, and in fact, can be assumed to be plug flow within acceptable error limits. The reactor used in this study was of such a type.

Assuming plug flow conditions then the equation describing the compositions is (18):

$$t = Ca^0 \int_0^{Xa} \frac{dXa}{-Ra} \quad (15)$$

for the reaction $A + B \rightarrow$ products, where t is the space time in the reactor at the point of consideration, Ca^0 is the point of concentration of reactant A, the halomethane in this case, Xa is the conversion of reactant A, expressed as:

$$Xa = 1 - Ca/Ca^0 \quad (16)$$

where Ca is the concentration of A at the point of consideration, and Ra is the rate of reaction with respect to A. The rate is expressed as:

$$-Ra = dCa/dt \quad (17)$$

For the primary reaction $H + CHCl_3 \rightarrow$ products, which is an ideal bimolecular reaction, the rate expression is:

$$dC_H/dt = -k * C_H * C_{CHCl_3} \quad (18)$$

The determination of k , the rate constant of the reaction, is one of the objectives of this study.

An initial model is developed and consists of 22 rate equations which are numerically integrated by Runge-Kutta 4th order method. The model is best fit to the data (conversion versus chloroform input concentration) using a Rosenbrock Hill Climb Algorithm.

(a) Runge-Kutta 4th order method

In the fourth-order method it is possible to develop one-step procedures which involve only first-order derivative evaluations, but which also produce results equivalent in accuracy to the higher-order Taylor formulas. Therefore, for the solution of the following system of n simultaneous first-order ordinary differential equations in the dependent variables Y_1, Y_2, \dots, Y_n :

$$\frac{dY_1}{dx} = f_1(X, Y_1, Y_2, \dots, Y_n),$$

$$\frac{dY_2}{dx} = f_2(X, Y_1, Y_2, \dots, Y_n),$$

(19)

$$\frac{dY_n}{dx} = f_n(X, Y_1, Y_2, \dots, Y_n),$$

with initial conditions given at a common point (X_0) , that is,

$$Y_1(X_0) = Y_{1,0}$$

$$Y_2(X_0) = Y_{2,0} \quad (20)$$

$$Y_n(X_0) = Y_{n,0}$$

the fourth-order Runge-Kutta method is applied for this study and the Algorithm is shown as follows:

(Runge-Kutta (order four) Algorithm)

To approximate the solution of the initial-value problem

$$\frac{dY}{dX} = f(X, Y) \quad a < X < b, \quad Y(a) = W_0$$

at $(N + 1)$ equally spaced numbers in the interval $[a, b]$: Input end points a, b ; integer N ; initial conditions 2.

Output approximation w to Y at the $(N + 1)$ values of X .

Step 1 Set $h = (b-a)/N$;

$$X = a$$

$$W = W_0 ;$$

Output (X, W) .

Step 2 For $i = 1, 2, \dots, N$ do steps 3-5.

Step 3 Set $K_1 = hf(X, W)$

$$K_2 = hf(X+h/2, W+K_1/2) ;$$

$$K_3 = hf(X+h/2, W+K_2/2) ;$$

$$K_4 = hf(X+h, W+K_3) ;$$

Step 4 Set $W = W + (K_1+2K_2+2K_3+K_4)/6$;

$$X = a+ih$$

Step 5 Output (X,w)

Step 6 STOP

(b) Rosenbrock Hill Climb Algorithm

This method is a sequential search technique which has proven effective in finding the maximum or minimum of a multivariable, nonlinear function subject to nonlinear inequality constraints:

Optimize $F(X_1, X_2, \dots, X_n)$

Subject to $G_k < X_k < H_k, k=1,2,\dots, M.$

Therefore, this method is applied for this study and the algorithm shown in Figure 2.

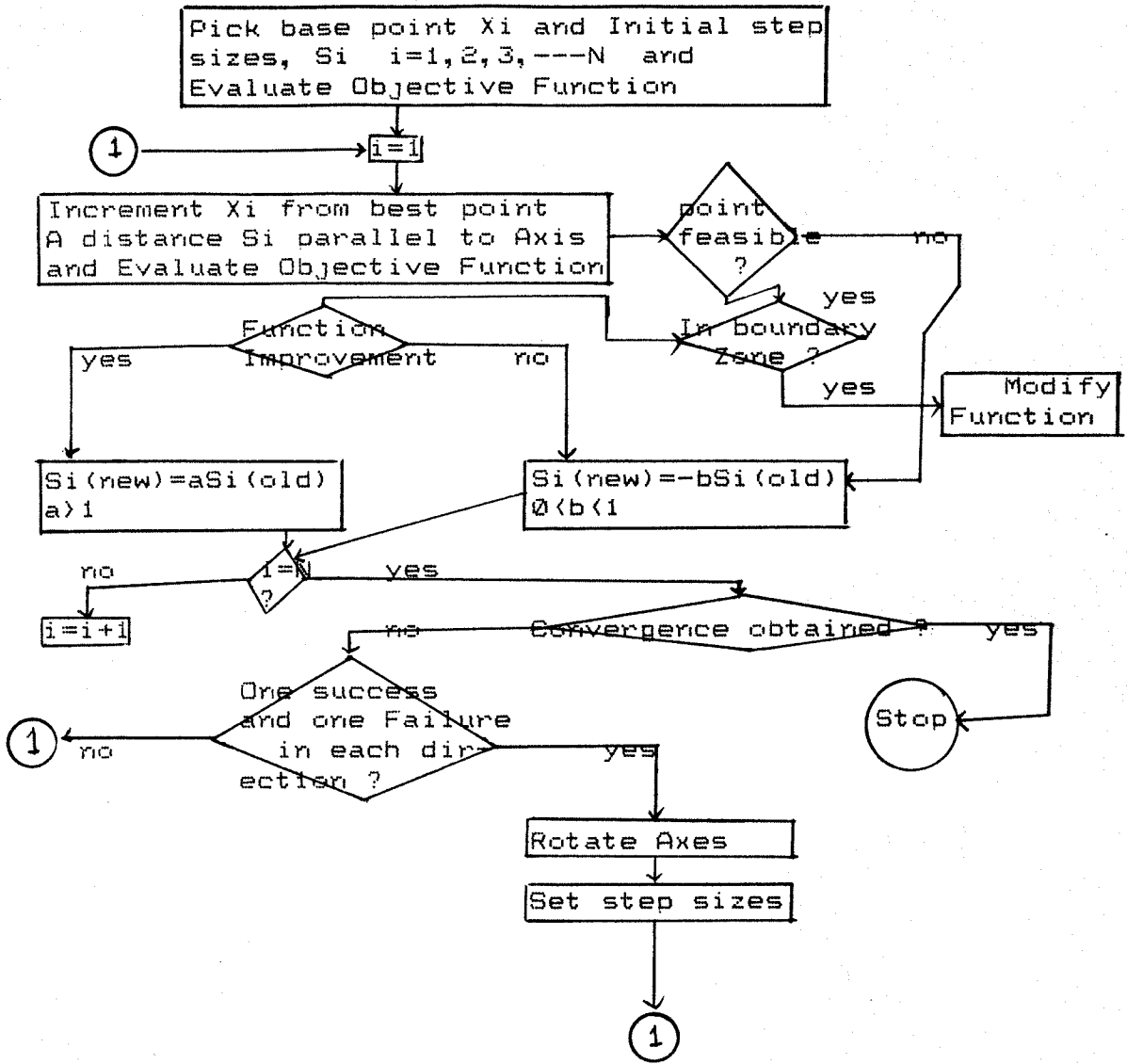


Figure 2. Constrained Rosenbrock (Hill Algorithm) Logic.

III EXPERIMENTAL APPARATUS AND PRODECURES

The experimental apparatus used in this study consists of a reactant gas inlet system, two flow tube reactors, each with a movable loop injector. In addition, a microwave-induced plasma discharge for hydrogen atom production, an ultraviolet-visible spectrometer and photomultiplier tube with a high voltage power supply and picoammeter with DC output for chemiluminescent measurements were used. A flame ionization detector gas chromatograph with sampling inlet was utilized for products analysis. A block diagram of the entire system is shown in Figure 3.

Since the first report of the dissociation of molecular hydrogen on hot tungsten filaments in 1911 (19), many methods have been developed for the generation of hydrogen atoms. The microwave discharge source has many attractive characteristics (20-22), principally it is electrodeless, radio-frequency (2450 MHz) and this microwave discharge was used for our study. The detection of H atoms and determination of their concentration has been made by both physical and chemical methods. Accurate measurements of the hydrogen atom concentration was a major problem, even though various methods were employed by previous researchers. Silver and de Hass (38), in their recent study of the reaction of $H + CF_3Br$, monitored the H atom Lyman-radiation, but their H atom concentration was of the order of 10^{12} atoms/cc, compared to more than 10^{14} atoms/cc in this study. Kleindienst and Finlayson-pitts (39) also dealt with low concentrations, and their method involved following the relative concentration of the

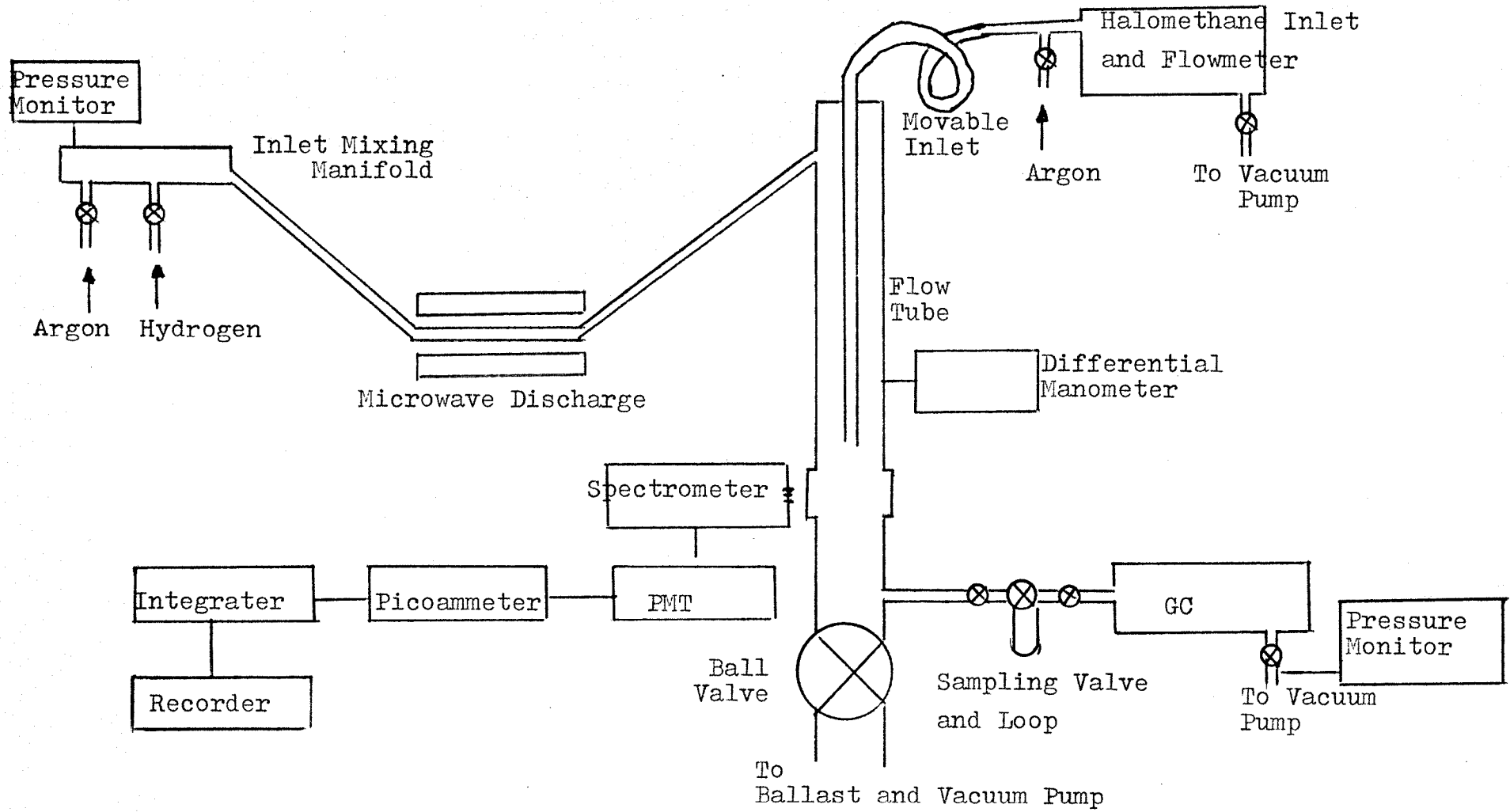


Figure 3. Experimental Setup.

hydroxide radical formed through:



Other studies, such as those of Westenberg and de Hass⁽⁵⁾ and of Ambidge et. al.⁽³⁰⁾ used integrated electron spin resonance spectroscopy.

In view of more sophisticated equipment and since the hydrogen atom concentrations were high, a method proposed by McKenzie et. al.⁽¹⁶⁾ was used to determine the hydrogen atom concentration in the present study. However, instead of using E.S.R. spectroscopy to monitor the $\text{H} + \text{NO}_2$ reaction, this research employed visible spectroscopy (chemiluminescence of $\text{H} + \text{NO}_2$).

Gases used in these experiments were prepurified argon gas from MG Industries, prepurified hydrogen and nitrogen gas from AIRCO Inc.. Argon and hydrogen gases were purified again in our system by passing through a Chemalog R3-11 oxygen removal catalyst and a molecular sieve trap for water removal, respectively.

All materials for the gas handling and flow system were constructed from Pyrex, stainless steel, tygon connectors, or Teflon. All glass stopcock valves were greased with low volatility Apiezon type M grease. In addition, the discharge tube and all tubes downstream of it were coated on the inside, with phosphoric acid (H_3PO_4) subject to evacuation and heating for water removal, to minimize recombination of hydrogen atoms on the walls. This was done by shaking and flowing aqueous solution of phosphoric acid in each tubes. The argon and the hydrogen

were then allowed to flow through the tubes for few days under vacuum (2 mmHg) to purge the H₂O as observed by the phosphoric acid was crystallized out as a layer on the inside of tubes.

Two flow tube were used for this study: both were Pyrex with one 4.0cm i.d and 1.0 meter length, and the other 2.6 cm i.d and 1.1 meter length. The vacuum pumping system allowed flow speeds of up to 4.18 m/sec in the 4.0 Cm ID reactor. Two Veeco TG-70 vacuum guages were used for pressure monitoring; one at the hydrogen-argon manifold and the second at inlet of small vacuum pump. An absolute Ar pressure manometer (oil 0.8 Sp.gr.) was positioned midway in the reactor-flow tube to measure pressure of the reaction system.

A ball valve was provided on the main flow tube 30 cm downstream of the spectrometer windows to regulate the flow, by throttling it, and to increase the reaction pressure in the flow tube as well as slowing flow (reaction time). The valve was made of PVC plastic, as also were the 1" I.D. tubing and elbows downstream of the reactor. To get a constant flame, not a flickering flame, a 35-liter stainless steel ballast was installed at the inlet of the pump to dampen the pulsations in flow caused by the pump.

Argon gas was passed first through an activated Chemalog R3-11 catalyst to remove any traces of oxygen in it. The hydrogen gas was passed through a molecular sieve trap to remove any water vapor impurity, and then sent to a manifold where it was mixed with argon. The R3-11 catalyst was activated by heating to 250° C under dry hydrogen flow. A calibrated differential pressure

flow meter (24) was used to measure the hydrogen flow, while the argon flow was measured by a calibrated rotameter. The dilute mixture of hydrogen in argon carrier gas, typically 0.74% hydrogen and 99.26% argon, then flowed through a 1" i.d. quartz tube placed in a microwave (20-22) at 2450 MHz to produce hydrogen atoms. The microwave power to the plasma is controlled and varied by adjusting the input voltage to a transformer supplying the full wave rectified magnetron power supply using a 0-120 volt variac. The discharge power could be varied approximately between 50 and 150 watts output power, and was normally operated at 50 watts.

The hydrogen and argon mixture then entered the reaction tube 50 cm above the spectrometer window. Argon was also passed through chloroform liquid trap and was bubbled in the trap to become saturated with chloroform vapor. Halomethanes vaporized with argon entered the flow tube through a movable teflon injector. The inlet position could be varied over 50 cm distance upstream of the spectrometer window. To improve mixing in the reaction zone, the inlet tube end was blocked off and six pinholes pierced along the circumference of the tube at a distance of 1.5 cm above the tip. This forced the halomethane to flow outward first, for mixing, and then downward with the bulk of the flow. Chloroform flows were determined by measuring the pressure increase in calibrated differential flow Meter (24).

A. Gas Chromatography

The gas chromatograph was a Varian Aerograph Series 1200 with a flame ionization detector (FID). The flame was provided by hydrogen gas at 30 cc/min flow rate, air and nitrogen carrier. Air from the laboratory supply compressed air line was passed first through an activated charcoal trap, to remove any organics, and then through a molecular sieve trap which absorbed any moisture present at 300 cc/min flow rate. Both traps were routinely activated by passing pure helium gas through while the traps were heated to 300°C in a furnace. Nitrogen gas was used without further purification at 30 cc/min flow rate as the sample and GC carrier gas.

The column in the gas chromatograph was a 6 ft. long 1/8" diameter stainless steel tube, filled with silicone oil SE-52, 5.0% on gas-chrom 60/80 mesh support. This column was maintained at 60°C when the halomethane used was chloroform. The column was routinely baked-out overnight at 130°C (with the carrier gas flowing through it) before a set of runs. The detector was maintained at 150°C and the output was sent to a 7155 B Chart recorder (HEWLETT PACKARD) with its range set at 0.5 MV per centimeter and a chart speed, 1.0 minute per centimeter.

A gas chromatograph was appended to the system to provide quantitative and qualitative analysis of the stable reagent and products in the reaction of atomic hydrogen with chloroform. Kinetic runs utilizing the gas chromatograph were started only after the reaction had stabilized, the ovens of the chromatograph reached their thermal equilibrium, and a steady baseline attached

on the gas chromatograph recorder. In addition, The reaction system was operated for about an hour after the reaction flame had been started and the flame of the flame ionization detector (FID) lit for equilibration before any measurements were made. At this stage, the pressure in the reactor was usually near 2.75 mmHg, and the pressure at the inlet of the sampling system vacuum pump normally was below 1 millitorr. This pressure gradient was essential to drive the sample through the sampling loop and the sampling valve.

Halocarbon analysis is introduced to the GC with 4-port Hamiltonian injection valve where the reactor, Pyrex 4.0cm I.D. and 1.0 meter length, is used. To see the effects of the reactor size on the reaction of the hydrogen atom with chloroform, another reactor which is of Pyrex, 2.6 cm I.D. and 1.1 meter length was also used with 6-port Hamiltonian injection valve in second experiment. A 1/4" diameter glass tube inserted 1.0 cm into the reactor center 20 cm downstream of the spectrometer window served as a sampling port. The tubing led to the gas chromatograph through 4-port and 6-port Hamiltonian injection valve respectively for each experiment. In sampling system, 1/4" and 1/8" stainless steel, teflon and glass tubing, and stainless toggle valves were used exclusively.

A schematic diagram of the sampling system is shown in Figure 4 for the 4-port and Figure 5 for 6-port Hamiltonian injection valve. As shown in Figure 4 and Figure 5, on-off valves were installed on the sample inlet line and the vacuum line. These were positioned as close to the sampling valve as

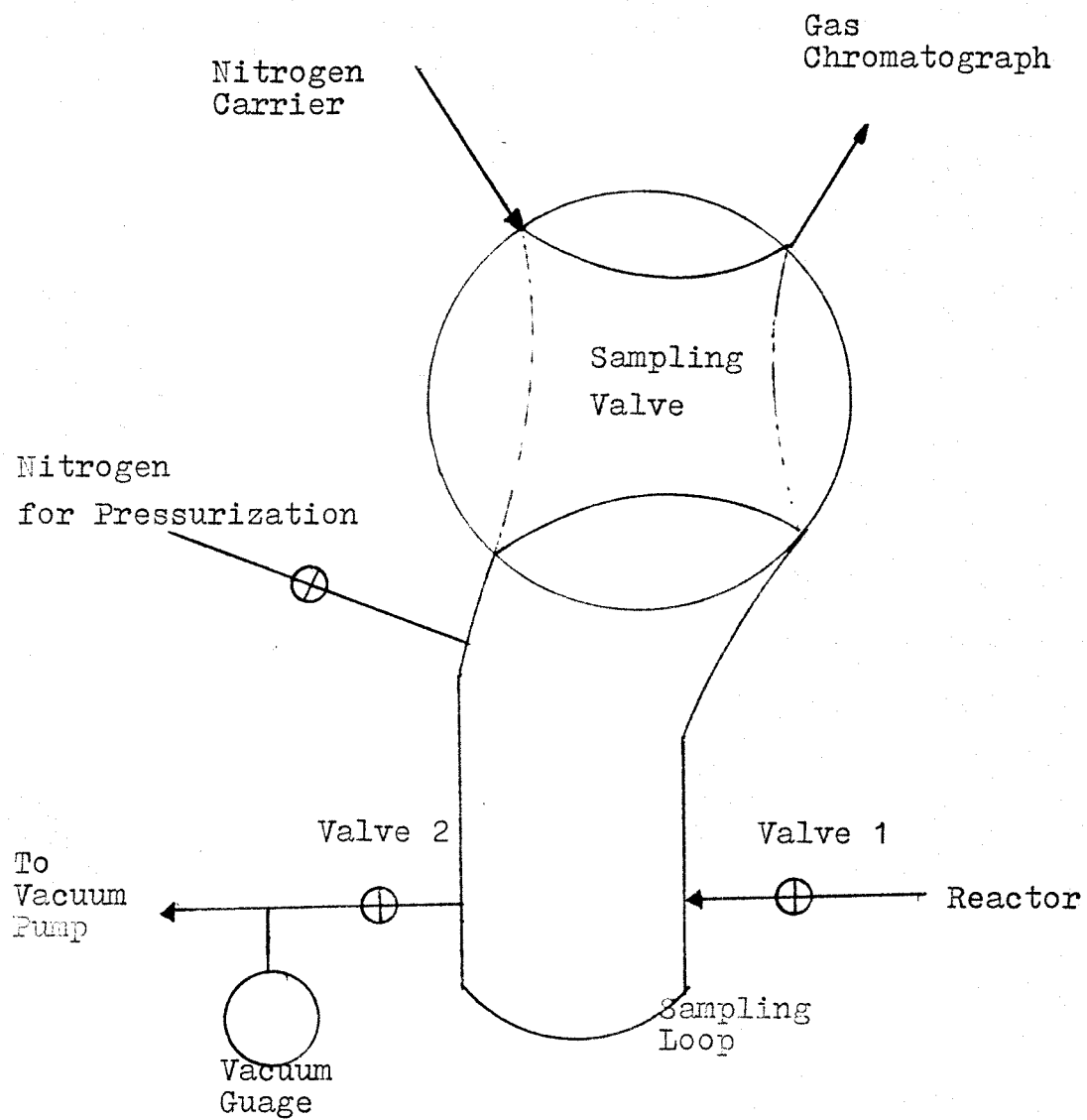


Figure 4. Schematic Diagram of the 4-port Hamiltonian Injection Valve .

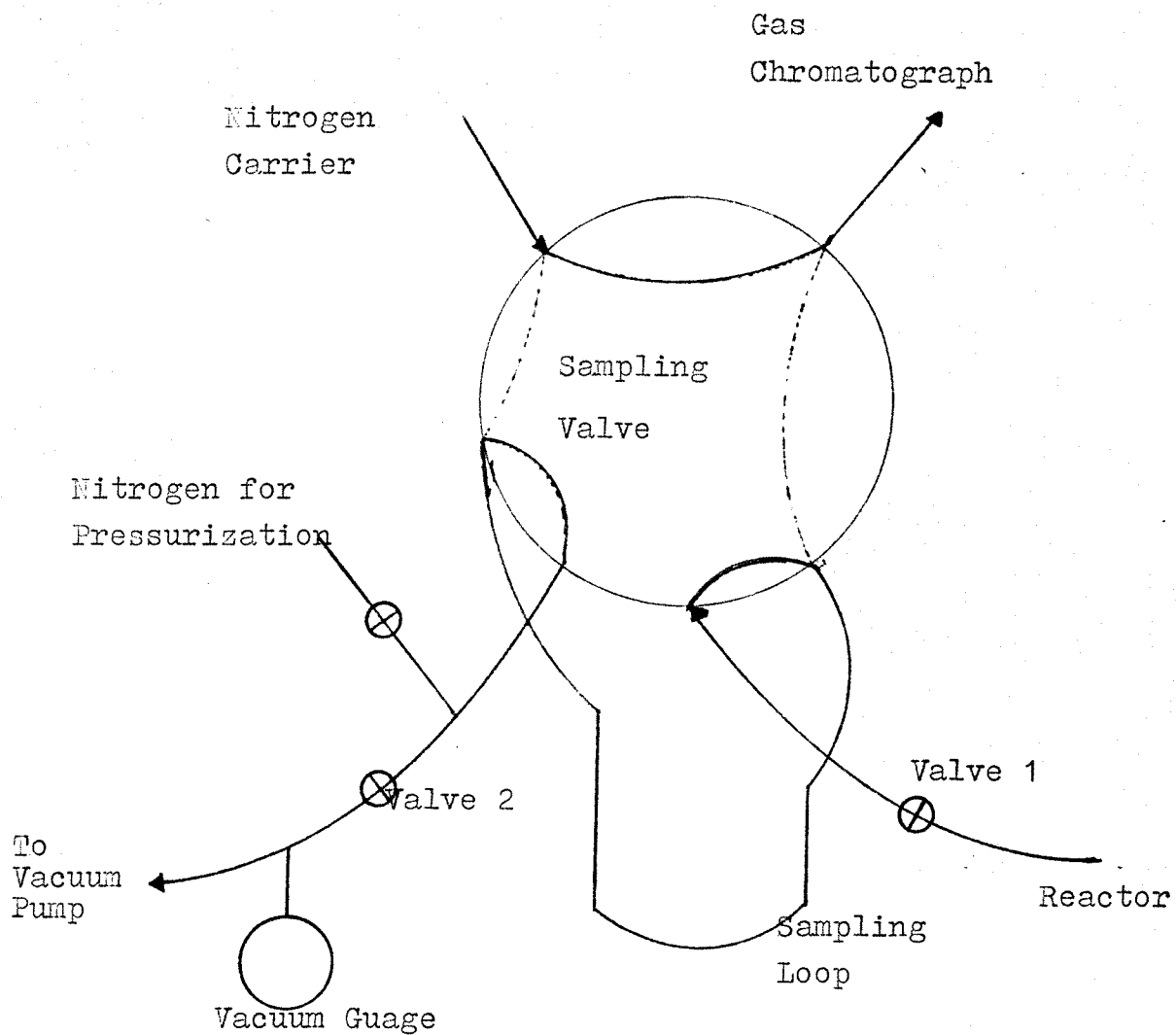
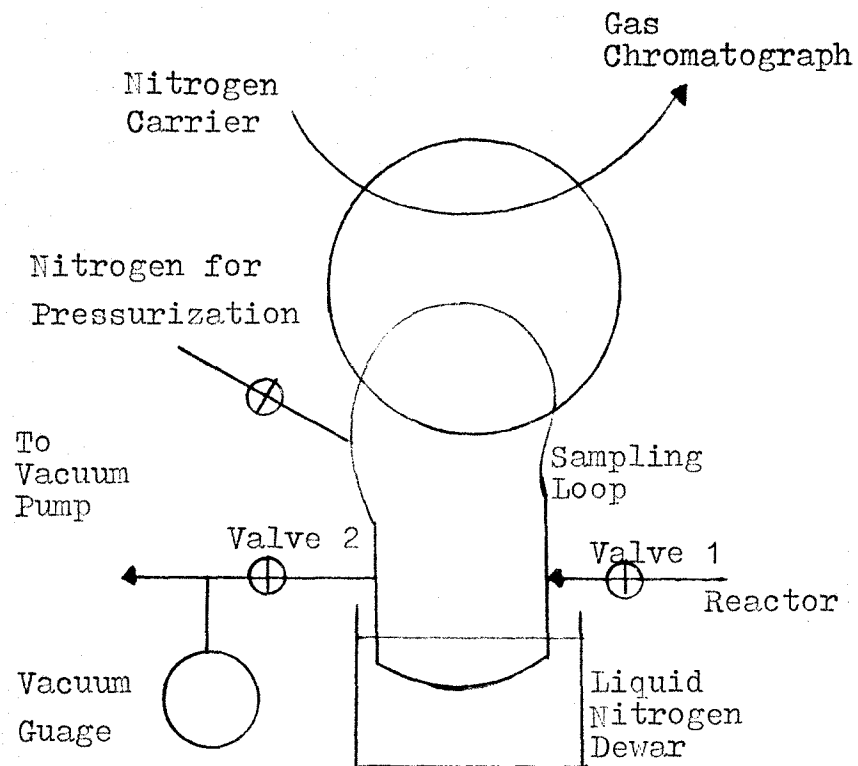


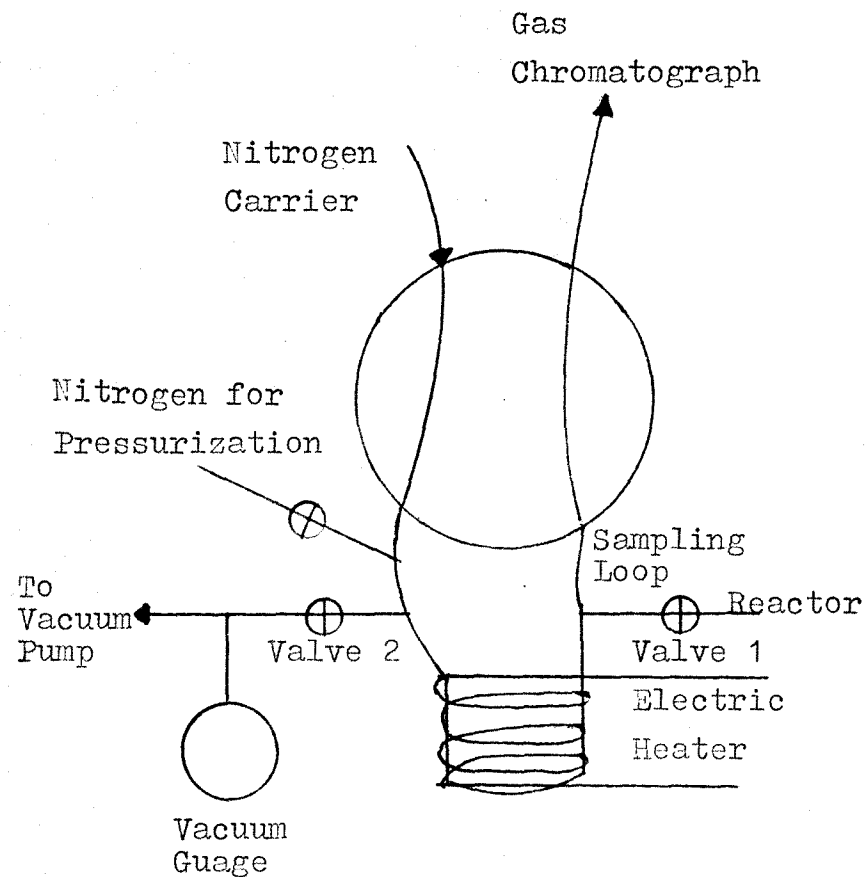
Figure 5. Schematic Diagram of the 6-port Hamiltonian Injection Valve.

possible to minimize dead volumes within the sampling system. Swagelok fittings were used for all intertubing connections to prevent any leaks into the vacuum. Furthermore, all stainless and glass tubing used in the chromatography section were cleaned first with detergent, then with acetone or methanol, and then oven-dried prior to installation into the system. The vacuum pump used in the gas sampling section of the apparatus was a Welch Scientific Model 1400. Pump oil was routinely changed for proper maintenance of vacuum. With no sample flowing--that is, with the inlet on-off valve to the sampling valve closed--this pump delivered a vacuum of below 1 millitorr at its inlet. Since the pressure in the reactor was normally around 2.75 mmHg, the pressure gradient of $(2.75-0.001)$ mmHg was the effective driving force pushing the sample through the loop. The sampling loop itself was a 48 cm long, 1/8" diameter stainless steel tubing, of which approximately 18cm length was in a liquid nitrogen bath for sample collection. This correspond to around 0.22 cm^3 of the loop within the trap out of a total of 0.59 cm^3 in the entire loop.

Operations of the 4-port and 6-port Hamiltonian injection valve were shown in Figure 6 and Figure 7, respectively, for collection and injection of a sample into the gas chromatograph. The sampling position, the on-off valve V1 at the sample inlet of the sampling valve was closed, and the on-off valve V2 at the vacuum end of the sampling valve was opened to evacuate the loop until the pressure gauge showed its lowest value--below 1 millitorr. Before sampling products, a liquid nitrogen dewar was

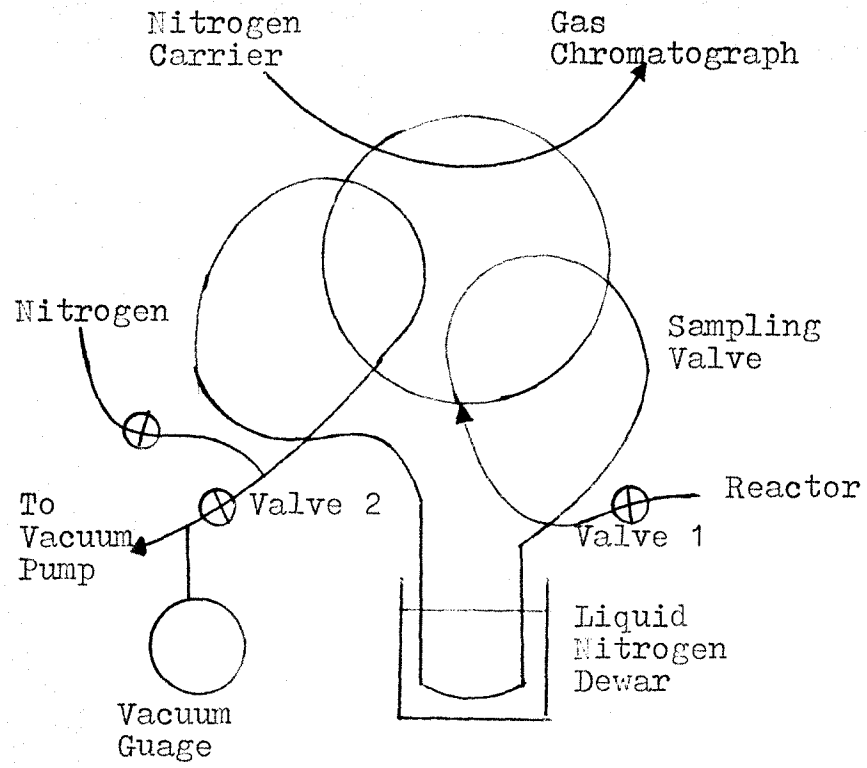


(1). Sample being collected

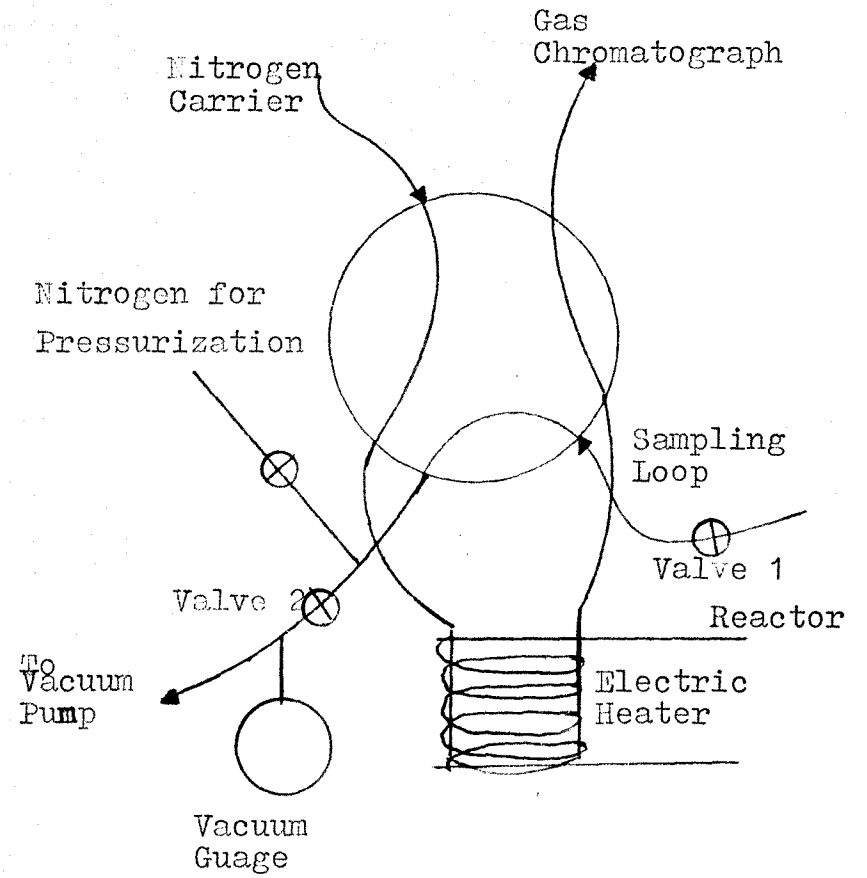


(2). Sample being injected

Figure 6. Operation of the 4-port Hamiltonian Injection Valve



(1). Sample being collected



(2). Sample being injected

Figure 7. Operation of the 6-port Hamiltonian Injection Valve.

placed under the loop before opening the valve V1, and the loop allowed to cool down to the liquid nitrogen temperature. Exactly after thirty seconds, the valve V1, was opened and the sample allowed to flow through the system for four minutes. as the sample flowed through the loop, the condensibles would collect and remain in the loop trap, but gases like hydrogen and argon would pass through it. To save experimental time, the sampling time was varied with flow rate of gases passing through the system at low flow rate, 4 minutes and at high flow rate, 2 minutes. After the proper sampling time, the valves V1 and V2 were closed simultaneously, and the liquid nitrogen dewar was then removed. Then the system was pressurized with nitrogen gas to improve the injection of samples collected in the loop to the column in the gas chromatograph. The pressurization was done by opening and closing the nitrogen valve for one second. Then, electric heating tape was slipped around the loop and heating started. The voltage heating the loop was fixed at 40 volts AC. Heating was done for exactly 3 minutes. When finished collection, sampling valve was switched to the injection position immediately. A stop watch was used for experimental time consistency in sample collection.

After the last of the peaks had been observed on the chromatograph and the peak data appeared on the recorder and integrator, the sampling valve position, and the valves V1 and V2 were opened again to evacuate the system for next collection.

Liquid nitrogen was used on both the Argon trap and hydrogen traps to check up the effects of liquid nitrogen which would

result in removing the impurities that might be contained in the Argon/Hydrogen gases on the reaction. This was done several times. No effects of this improved liquid nitrogen trap for purification were observed on the reaction, indicating that the observed reactions were results of H atoms and chloroform and nitrogen or oxygen atoms were not present in reaction.

To insure consistency in the data obtained, all experimental runs were done with exactly the same time interval for each operation.

B. Titration of Hydrogen atoms

The spectrometer used to monitor chemiluminescence for titration of hydrogen atoms was a McKee Pedersen 0.47 meter spectrometer fitted with a Jarrell Ash grating blazed at 350 nm, and containing 1300 lines per millimeter. This spectrometer was coupled with a side-on type photomultiplier tube (PMT), a Model R928 by Hamamatsu. The signals from the PMT were input to a high voltage power supply (Model 228 by Pacific Photometric Instruments) and then to a Keithley 480 high-speed Picoammeter which showed the current intensity in digital output. The spectrometer was capable of 0.01 nm resolution, and allowed scanning rates of 2 to 10 nm per minutes. The spectrometer was calibrated using mercury and sodium vapor lamps on the standard lines of 253.7 nm, 366.3 nm, and 589.6 nm for sodium (25). Besides the inlet of spectrometer window at the flow reactor, a black cloth was wound around the entire flow reactor to prevent it from reflecting by light. The PMT used in this study, a Hamamatsu R982, had a spectral range of 200-800nm. The slit at

the spectrometer was controlled to a desired value--usually less than 5000 microns. Higher slit widths gave higher PMT current but lower resolution. Often a compromise had to be struck between these two parameters when deciding upon a slitwidth. Care was taken, however, to prevent opening the slitwidth to such an extent that the PMT current was greater than 1 microampere, at which level the PMT could be damaged. For especially strong flames the bias to the PMT, normally at 1KV, could be reduced to decrease the PMT current. With this knowledge the slit was adjusted to the least opening, 4800 microns in this study that gave proper intensity of picoammeter in the whole range desired. Flowing across the titration range was then repeated at a desired flow rate to obtain an idea of the magnitude of the emission intensities. Since the intensity of output is directly related to the current in the picoammeter, this current was read directly off the picoammeter, choosing the required ampere range. This allowed for meaningful comparison of all intensities on one scale.

The hydrogen atom concentration in the reactor flame was measured by chemiluminescence titration with nitrogen dioxide. The NO₂-Argon mixture (16% of NO₂ and 84% of argon) was made up in a 35 liter stainless cylinder to a pressure of 30 PSIA. The NO₂-Argon mixture entered the halomethane system manifold after its flow was monitored on a calibrated rotameter. The flow was controlled by a needle valve installed on the line between the rotameter and the manifold. The mixture was inlet through injection tube, same as chloroform, which was now closed off.

The microwave discharge was turned on, making sure that the discharge coolant fan was running, the housing (cavity) around the flow tube in the discharge was not overheated by the microwave system. The flame in the flow tube was purple at each running of the microwave. The Variac supplying the voltage to the microwave was first set at 100 volts to start the plasma and after 30 seconds at 90 volts for all experiments. The atomic hydrogen produced by the discharge was allowed to react with the impurities absorbed on the walls of the reactor, and thus clean the reactor. Then a dilute mixture of NO_2 in argon (about 16% NO_2 by volume) was allowed to take the path normally taken by the halomethane to keep same experimental conditions, and the resulting HNO^* flame at the tip of the injector tube in the flow reactor was studied.

The flame caused by the reaction of hydrogen atoms with NO_2 was scanned in the range 300-800nm. As noted earlier, a large band was found in the region of 686.5-698.5 nm (15), and the largest signal in this range determined our titration wavelength. The NO_2 -Argon mixture was then varied for observation of the intensities of HNO^* at various flow of NO_2 -Argon mixture. The effect of this parameter on the intensity of emission of HNO^* at 292.8 nm was monitored. The titration itself was performed by observing the digital signal resulting from the picoammeter current, as a function of the NO_2 flow (cc/sec.).

Before any readings were taken, the system was conditioned by running for about one hour to get consistent results in the spectroscopic analysis of the reaction. To focus the light from

the reaction flame into the spectrometer, aluminum foil was wrapped around reaction tube at the level spectrometer window.

IV. RESULTS AND DISCUSSION

A. Experimental Results

For qualitative and quantitative analysis a gas chromatograph was attached to the system in this study. Although there were species present in the reactor that were "active" and emitting radiation, it must be noted that all such species are "consumed" or "die" within a short distance into the GC sampling tube, presumably by wall loss. Thus the gas chromatograph analyzes only the stable end products.

The GC peaks were qualitatively identified by injecting the pure compounds separately through a septum and observing the peak response time for each compounds. After identifying the GC peaks qualitatively by preliminary experiment, experiments wanted were done. Data were first obtained for eight different chloroform concentration at a constant hydrogen flow and the whole experiment repeated five times for five different hydrogen flows at each other chloroform flows. The experiments were also performed for two different reaction time at eight chloroform flows in a seperate kinetic experiments. The results of all experiments are given later.

All experiments were run in the following manner: the CHCl_3 flow was set at a value that gave a bright flame. This was easy to do because the flame became brighter as the flow was increased to a point, beyond which it became less bright.

Liquid nitrogen was placed around the argon/hydrogen traps to check on the effects of removing oxygen, nitrogen and other impurities that might be contained in the argon/hydrogen gas cylinder. No effects of the liquid nitrogen trap for purification were observed on the reaction or emission flame with trapping for several hours.

The flow rate of CHCl_3 was measured by the capillary flow meter and the flame resulting from the reaction of hydrogen atom with chloroform allowed to stabilize for a 30 minutes before the run was started. The sample was collected and injected following the procedure detailed in Chapter III. The runs were repeated with and without the microwave discharge for determining of the conversion of chloroform, through the relation:

$$X = 1 - \frac{\text{Area under CHCl}_3 \text{ peak in sample with reaction}}{\text{Area under CHCl}_3 \text{ peak in sample without reaction.}}$$

This technique was considered more accurate than the one that involved the measurement of the area of CHCl_3 as a fraction of the total area under the various peaks in the reaction sample. It was felt, however, that there was scope for error in the collection efficiency of the trap as regards all products, specifically methane. After completing the two runs--with and without reaction--at a given halomethane flow rate, the flow of the chloroform was measured again to check for errors before the next flow rate was tried. The above procedure was then repeated. The results of the experiments are shown in Figure 8 and Figure 9. The discussion of these results is shown in the computer

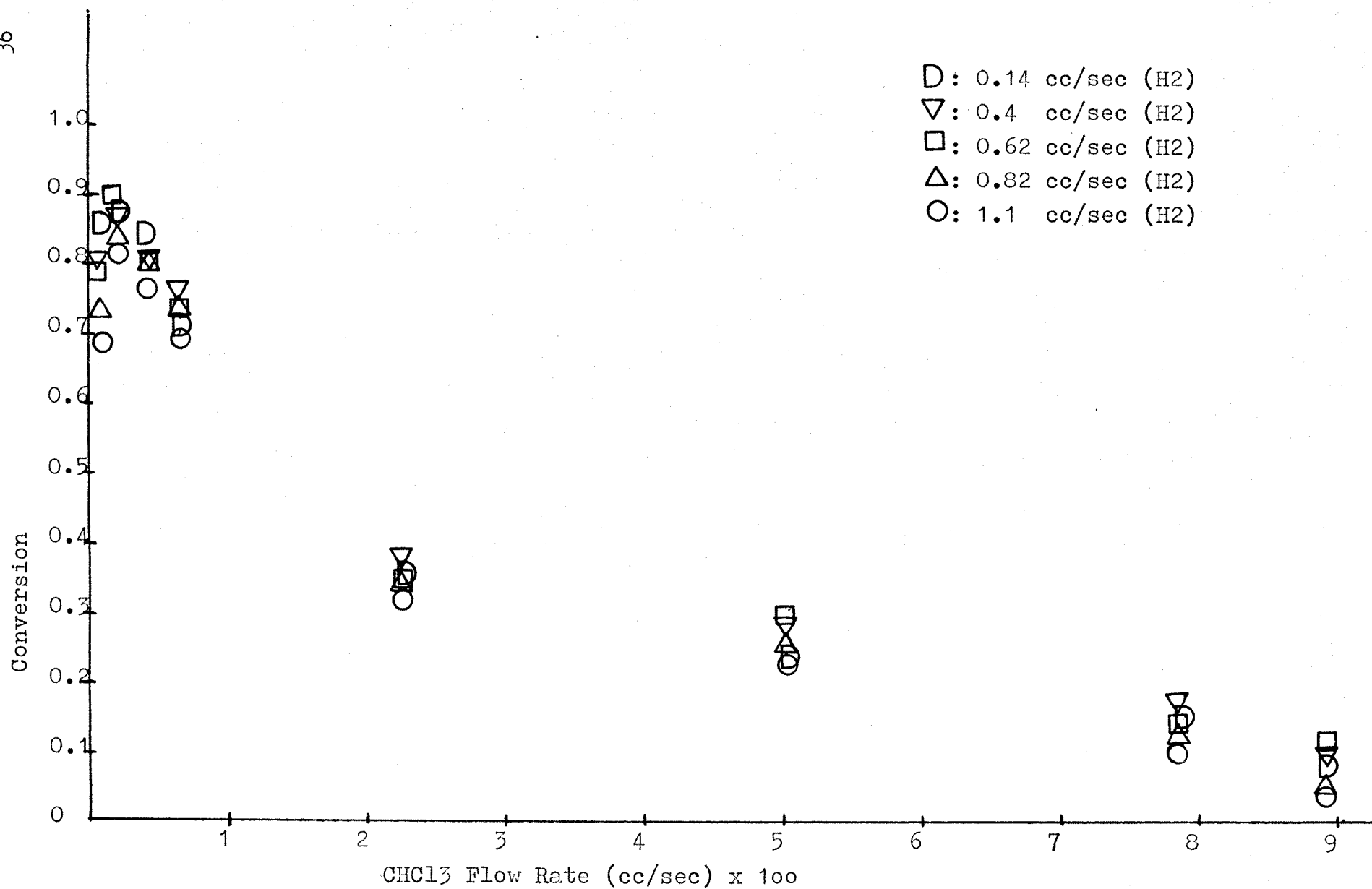


Figure 8. H-CHCl₃ Experimental Curves at Five Different H₂ Flow Rate.

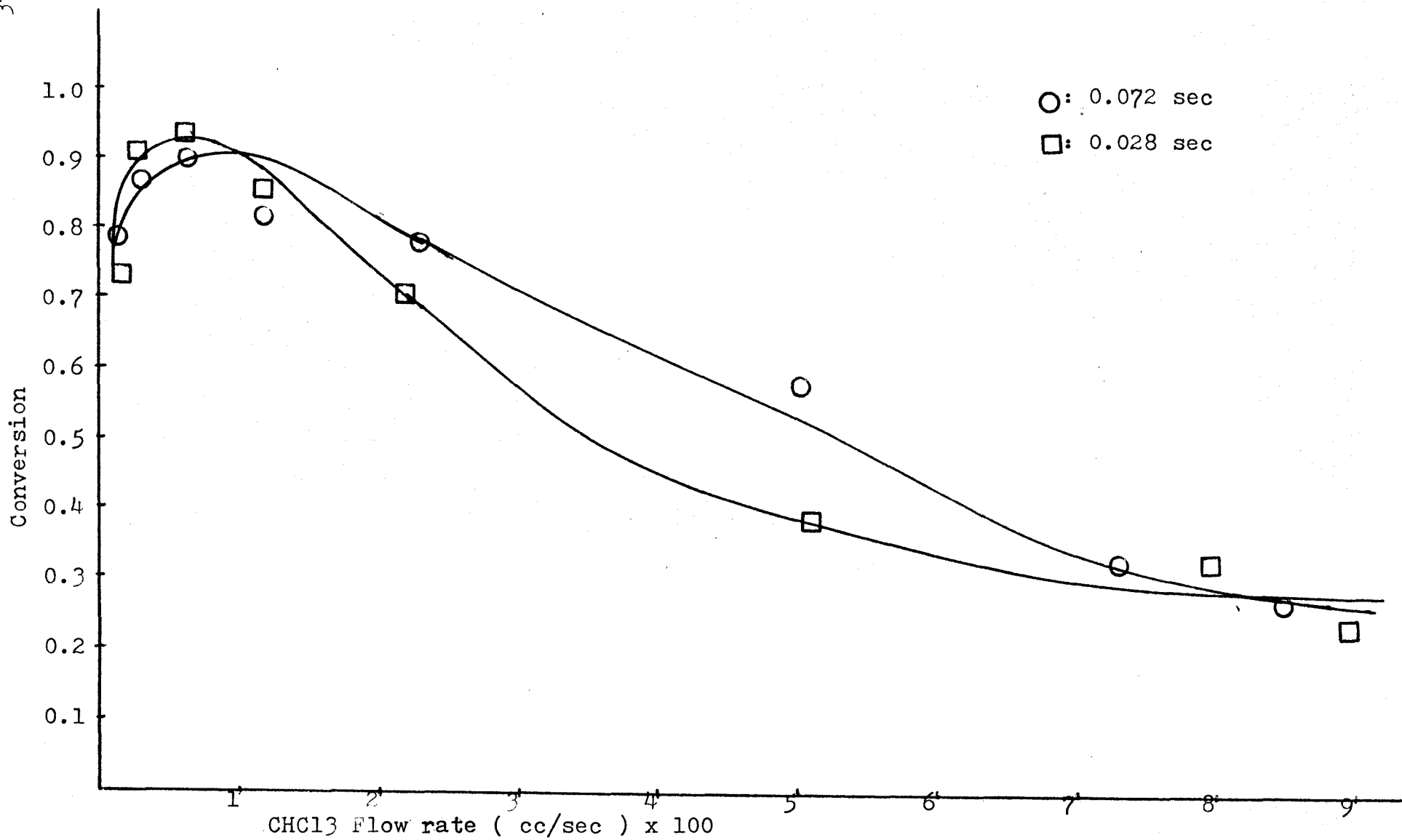


Figure 9. H-CHCl₃ Experimental Curves at two different Reaction Time.

modelling and discussion section. A reaction mechanism is compiled first to find the unknown rate constant of H-CHCl₃ reaction by comparing experimental results with a computer model.

B. Hydrogen Atom Concentrations.

The determination of reaction kinetics requires the knowledge of the exact concentrations of reagents entering the reaction zone. In this experiment, though the H₂ flow rate into the system is known, as yet there had been no estimate of the H atom concentrations. This was determined by titration of hydrogen atoms against nitrogen dioxide. The principle on which this method is based has been detailed earlier in Chapter II.

In the hydrogen atom titration experiments, NO₂ (16.25%) mixed with argon gas (83.75%) were introduced into the halomethane manifold to flow into the reactor through the Teflon injector under identical experimental conditions as that of chloroform in the reaction process. This way the NO₂ encountered the same hydrogen atom concentration and flow tube conditions as did the chloroform. As the NO₂ flow was varied the intensity of the HNO* emission produced was monitored at a wavelength of the most intense signal in the present work, Makee Pederson 1/2 meter monochromator with slit width 4800 um. The six different resulting curves were shown in Figures 10, 11, and 12 for the six different flow rates of hydrogen.

As the figures indicate, the intensity of the HNO* emission goes through a maximum before decreasing rapidly. A tangent was drawn at the point of the maximum negative slope and extrapolated to the X axis to determine the NO₂ flow rate that corresponded

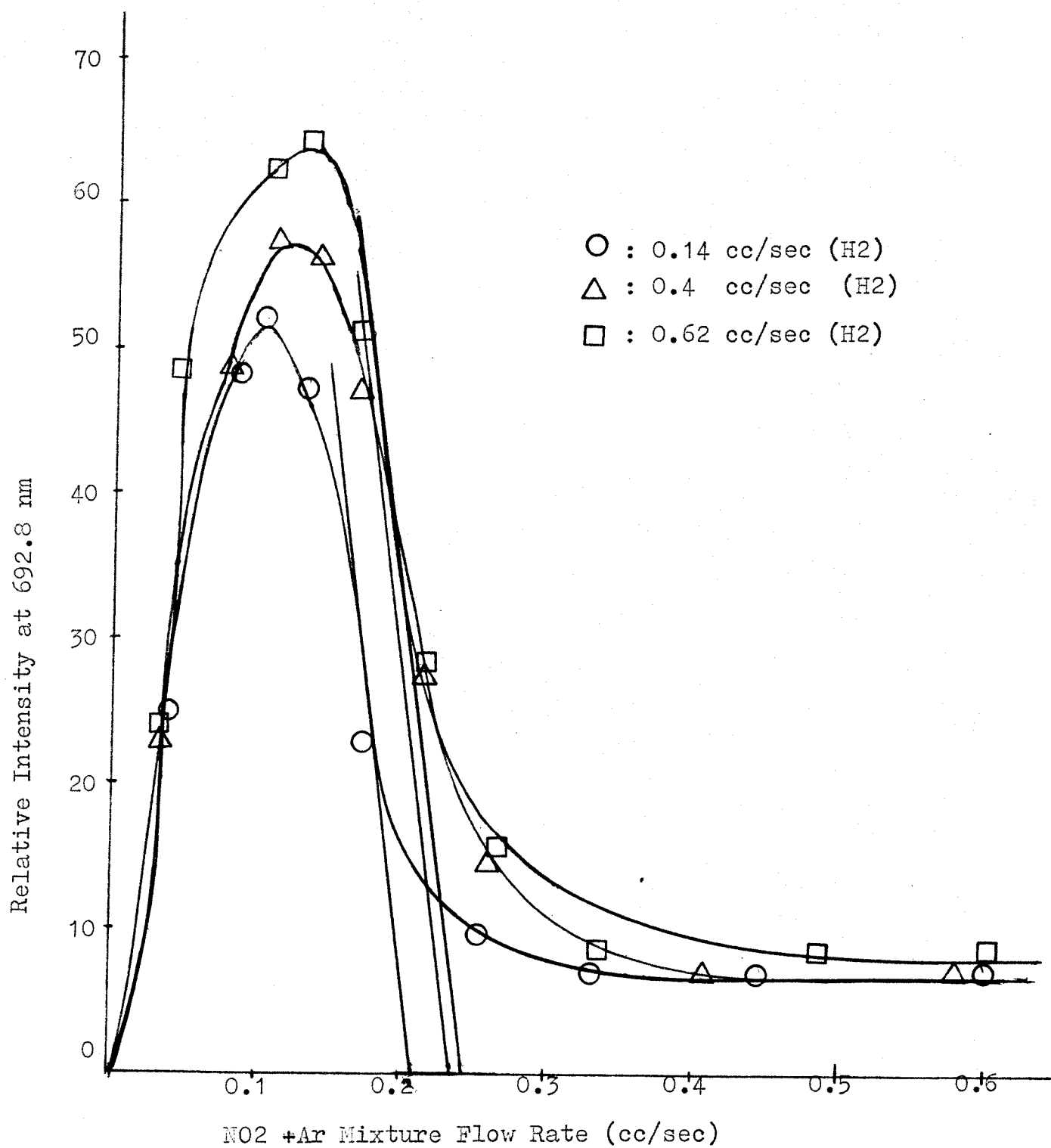


Figure 10. Hydrogen Atom Titration Curves with NO₂.

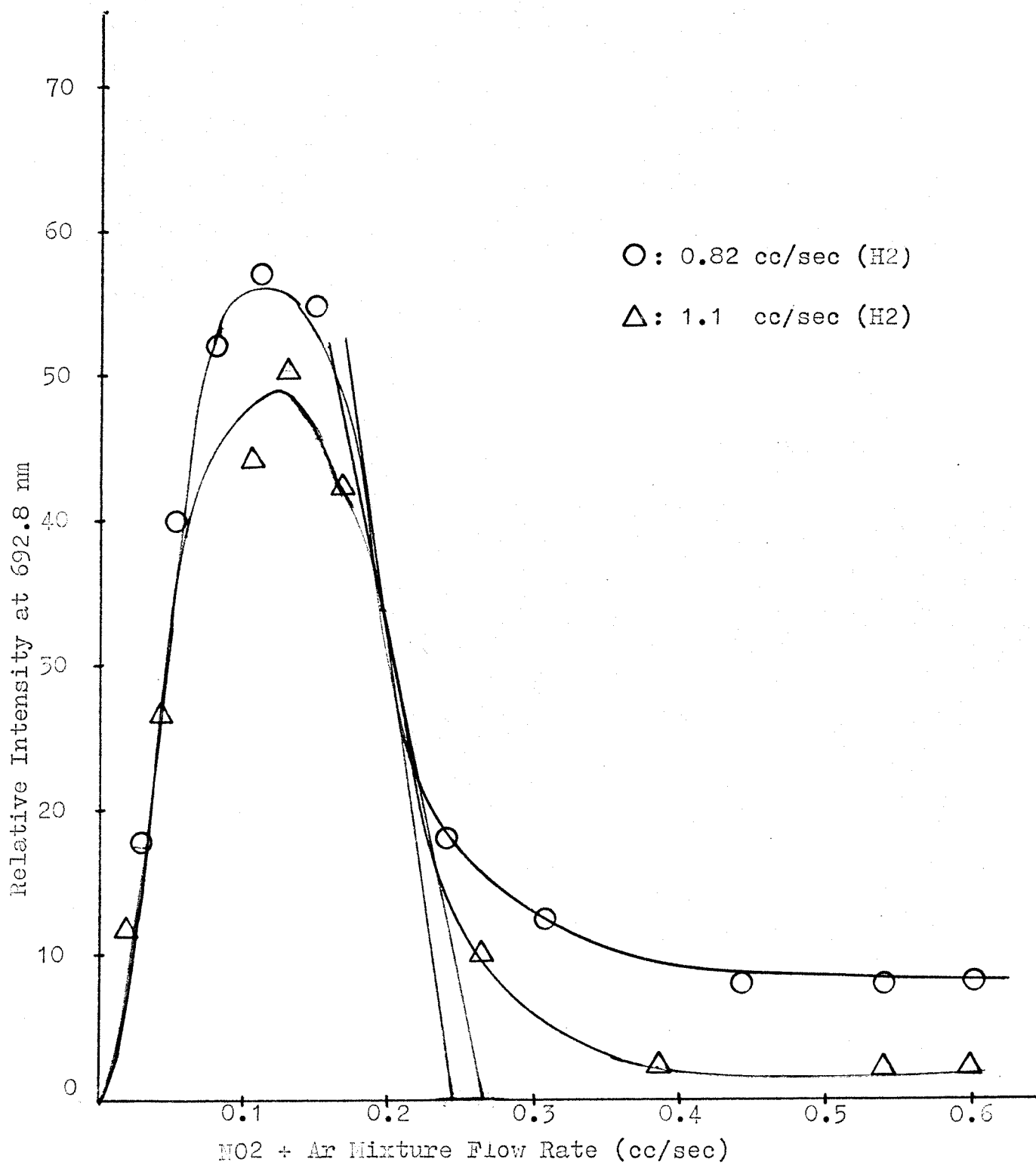


Figure 11. Hydrogen Atom Titration Curves with NO₂.

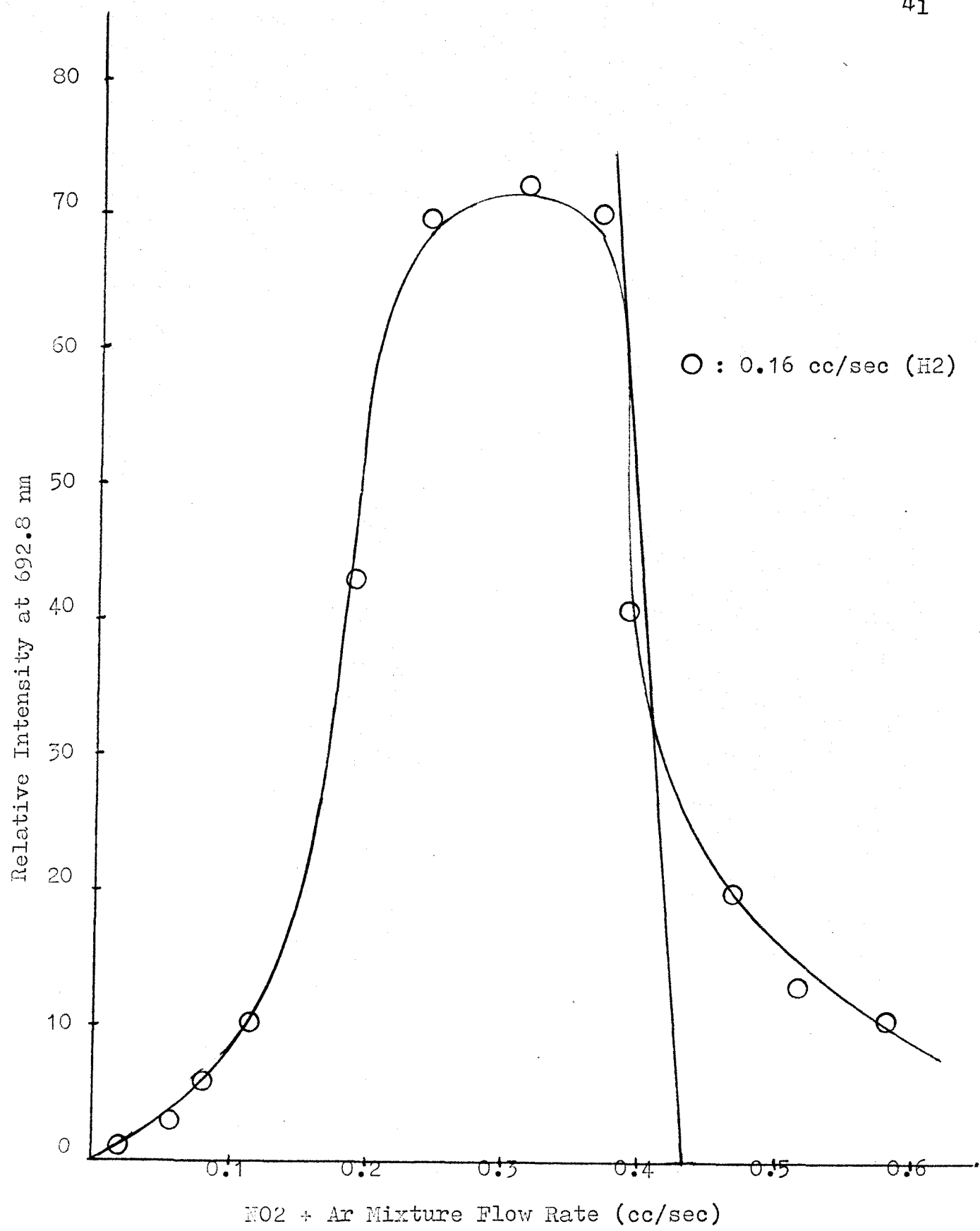
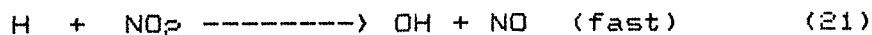
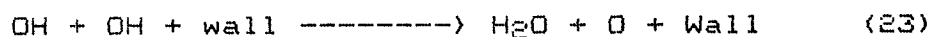


Figure 12. Hydrogen Atom Titration with NO₂.

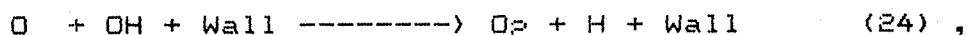
to the end point of the titration. A 1:1 stoichiometry of nitrogen dioxide and hydrogen atoms leads to the following reactions:



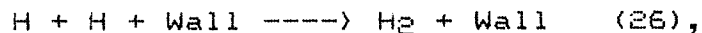
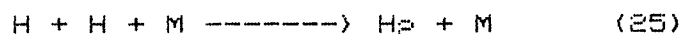
When NO_2 concentration is equal to that of hydrogen atoms there will be no hydrogen atoms left to react with NO to form HNO^* . The wall effect was carefully considered in terms of two factors in this study. One of them is, by McKenzie et. al. (16), that the concentration of NO_2 required precisely to consume an hydrogen concentration, $[\text{H}]$, can vary from about $1.1[\text{H}]$ to $1.5[\text{H}]$ depending on the activity of the wall, due to the following subsequent two reactions:



and



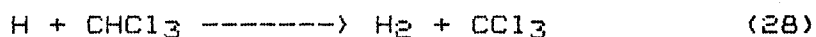
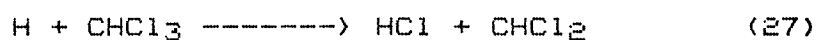
where the OH 's produced by the reaction (21) react with each other and subsequently, with the oxygen atom produced by the titration reaction (23). The other is that as the inlet flow of H_2 is increased there is only a very slight increase in the hydrogen atom concentration, depending on the efficiency of the molecular hydrogen dissociation, and the molecular hydrogen concentration increases more rapidly. The following reactions are possibly the reasons for the rapid increase in the H_2 concentration:



which hydrogen atoms produced recombine. For these two factors, the wall of reactor was coated well with phosphoric acid and so, the wall effect is minimized and insignificant as demonstrated by results of hydrogen atom concentrations at top and bottom of the flow tube. The calculations of the hydrogen atom concentration from the experimental data are shown in Appendix 4.

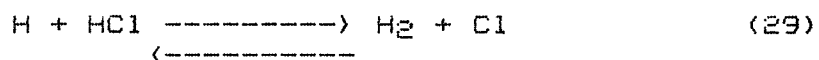
C. Reaction Mechanism

It is known that the primary reactions are reaction 27 and reaction 28 by the occurrence of halogen-atom abstraction and hydrogen-atom abstraction, respectively.

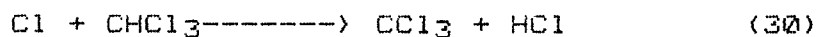


Results of Gould et. al. show that the probabilities of Cl abstraction is 7.2 times larger than that of H abstraction.

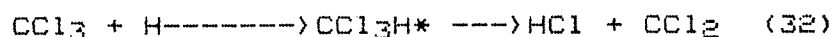
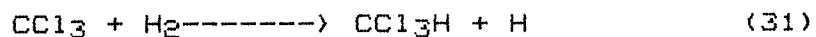
The reaction 29,



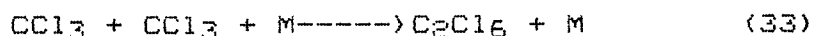
has been studied for nearly a century. Despite the intense effort to understand this elementary system, there were several different rate constants for this reaction (26-30) until most recently, Miller and Gordon (31) studied the reaction and found the rate constants for this forward and reverse reaction and compared them with other's in the literature. Therefore, Miller and Gordon's rate constants for reaction 29 are used in this study. Watson (28) and CLYNE, et. al. (29, 32) have shown the occurrence of the reaction:



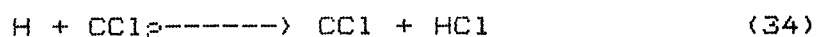
where an increase in the HCl concentration would then have decreased the CHCl₃ consumed. The CCl₃ formed in reaction 30 has three possible reactions open to it (33).



and



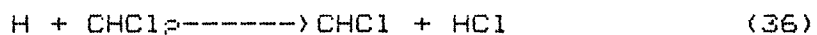
of these, the first reaction is endothermic to 14 Kcal/mole, and, therefore, insignificant at 298°K. In addition, the absence of chloroethanes in the products precludes the possibility of reaction 33 occurring in our system, leaving reaction 32 as the predominant reaction. The same pattern is conjectured to follow in the further reactions of CCl₂:



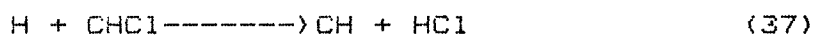
and



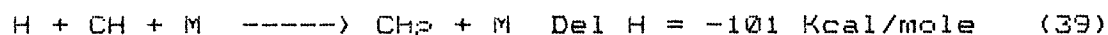
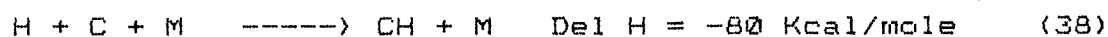
The CHCl₂ molecule that is formed by reaction 27 is again subjected to chlorine abstraction by the hydrogen atoms (33):

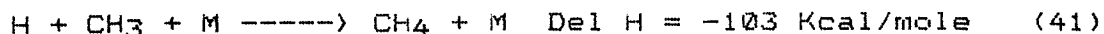
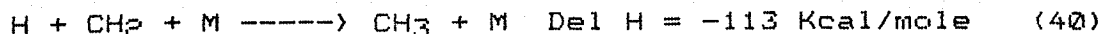


and

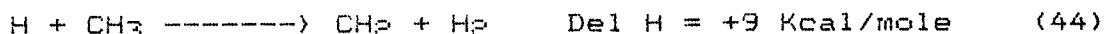
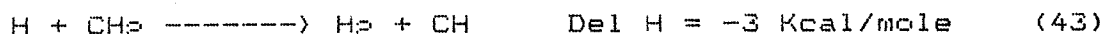
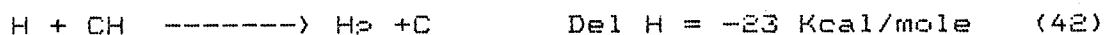


With the formation of the carbon atoms produced by the reaction 35 as observed in Chari's studies and on tip of the movable injection tube in this study, a series of recombinations are required to produce methane, which was observed on the chromatogram. The most likely reactions for formation of methane then are the trimolecular reactions (34):



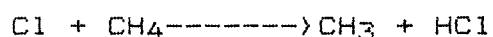


where M is likely to be argon, the species most abundant in our system. Other possibilities for the consumption of CH and CH₂ are:



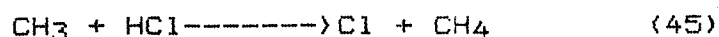
The reaction 42 as well as reaction 45 is exothermic, but Del H in reaction 39 is 4.4 times more exothermic than that of reaction 42 and the rate constant for reaction 39 is 2.41×10^{-14} cc/molecule-sec (35), compared to 2.67×10^{-17} cc/molecule-sec for reaction 42. The rate constant for reaction 40 is not available, but the trend may lead one to the conclusion that the rate constant for reaction 40 is much higher than that for reaction 43. The reaction 44 is endothermic and is not preferable for this study. Therefore, it is the trimolecular reactions 38-41 that are likely to occur, even though intuition seems to suggest otherwise --- for these reactions require the presence of a third body at the collision site on time. Since the reactions 38-41 are very similar, the rate constants for all these reactions have been taken as 2.41×10^{-14} cc/molecule-sec, which the value of k_{39} (35).

Once the methane is formed, it may react with any of the chlorine atoms still present by the reaction:

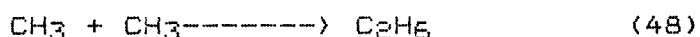
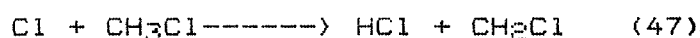
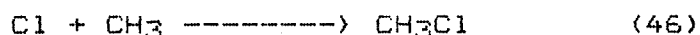


which is well-studied (29), and whose rate constant is known to

be 1.25×10^{-13} cm³/mol sec at room temperature. Furthermore, its reverse reaction,



is shown in Weissman and Benson's study (36) and rate constant for this reaction is calculated, using their thermochemical data. Owing to the very low concentration of the chlorine atoms due to reverse of reaction 29 in excess H₂, and the reverse of reaction 45, this reaction is highly unlikely, but has still been included all reactions as possible. The other possible reactions 46-50 (36),



are also included in the computer model and their rate constants are calculated using Benson's thermochemical data even though the extent of the reactions is small due to low Cl concentration from the reaction 29 because excess H₂ shifts equilibrium.

The only other reaction we considered of importance is the H atom recombination reaction:



with a value of 1.54×10^{-15} cm³/sec (35), k_{51} is small enough not to seriously affect the reaction scheme, but has been accounted for in the computer model since changes in H atom concentrations are influential in deciding the extent of many of reactions considering here.

The appendix 3 lists all the reactions considered in the overall reaction mechanism and the rate constants at 298°K.

D. Computer Modelling and Discussion

The Kinetics of the reaction system were simulated on the UNIVAC 90/80-3 system for the reaction of hydrogen atom with chloroform. Using the modelling technique described in Theory section, a computer model incorporating the various reactions in the reaction mechanism was formulated. Appendix 4 shows the procedure of calculation of hydrogen atom and chloroform concentration. Appendix 5 contains a compilation and results of the program written for the reaction of hydrogen atom with chloroform. The only rate constants not available at this stage were: i), for the primary reaction, as described by reaction 27, and ii), for the reactions 36 and 37. For the reactions 36 and 37, there was no data available, but the rate constants were assumed to be of the order of 1.0×10^{-11} cm³/mol sec. because both the reactants in each of these reactions were reactive radicals, as reactions 32, 34 and 35. With this assumption it, the rate constant for the primary reactions was obtained by computer modelling is to obtain the rate constant for the primary reaction 27, which best fits the experimental results.

The CPU time, when the Runge-Kutta fourth method only was used for solving the 22 consecutive differential equations, was 50 to 100 seconds. When the results from Runge-Kutta Method was compared with those from simple Euler integration method, there was no difference between them, demonstrating consistency in the computer program. A Rosenbrock Optimization was added in the

program to obtain the rate constant unknown, The Runge-Kutta Fourth Method with the Rosenbrock Optimization Method for this study gave the CPU time, 200-300 seconds which were three to four times longer than those when Runge-Kutta Forth Method only was used. In applying the Rosenbrock Optimization Method for computer Modelling, much care was needed in choosing an initial value of k_{27} because it would give over flows or under flows in the computer calculation due to the improper initial value.

The results from computer modelling are shown in Figures 13 to 19, separately. As shown in figures 13 to 19 in the conversion curve for changing the flow rate of chloroform the extent of conversion increases first to a point and then decreases. This indicates that though the conversion of chloroform is increased at low CHCl_3 concentration as the flow rate of chloroform is increased, while at higher CHCl_3 values it is limited by the hydrogen atom concentration. The initial $[\text{H}]$ is unchanged through one whole experimental series of CHCl_3 flows. Therefore, the hydrogen atom concentration becomes the limiting factor for the conversion of chloroform at higher CHCl_3 concentrations.

As shown Figures 13 through 17, the conversion curves are almost same at five different hydrogen flow rates which have only slightly different hydrogen atom concentrations, and all other experimental condition were constant. There was strong flame during hydrogen atom titration. For these results, the rate constants which were obtained by computer modelling were compared with each other. It can be seemed that the rate

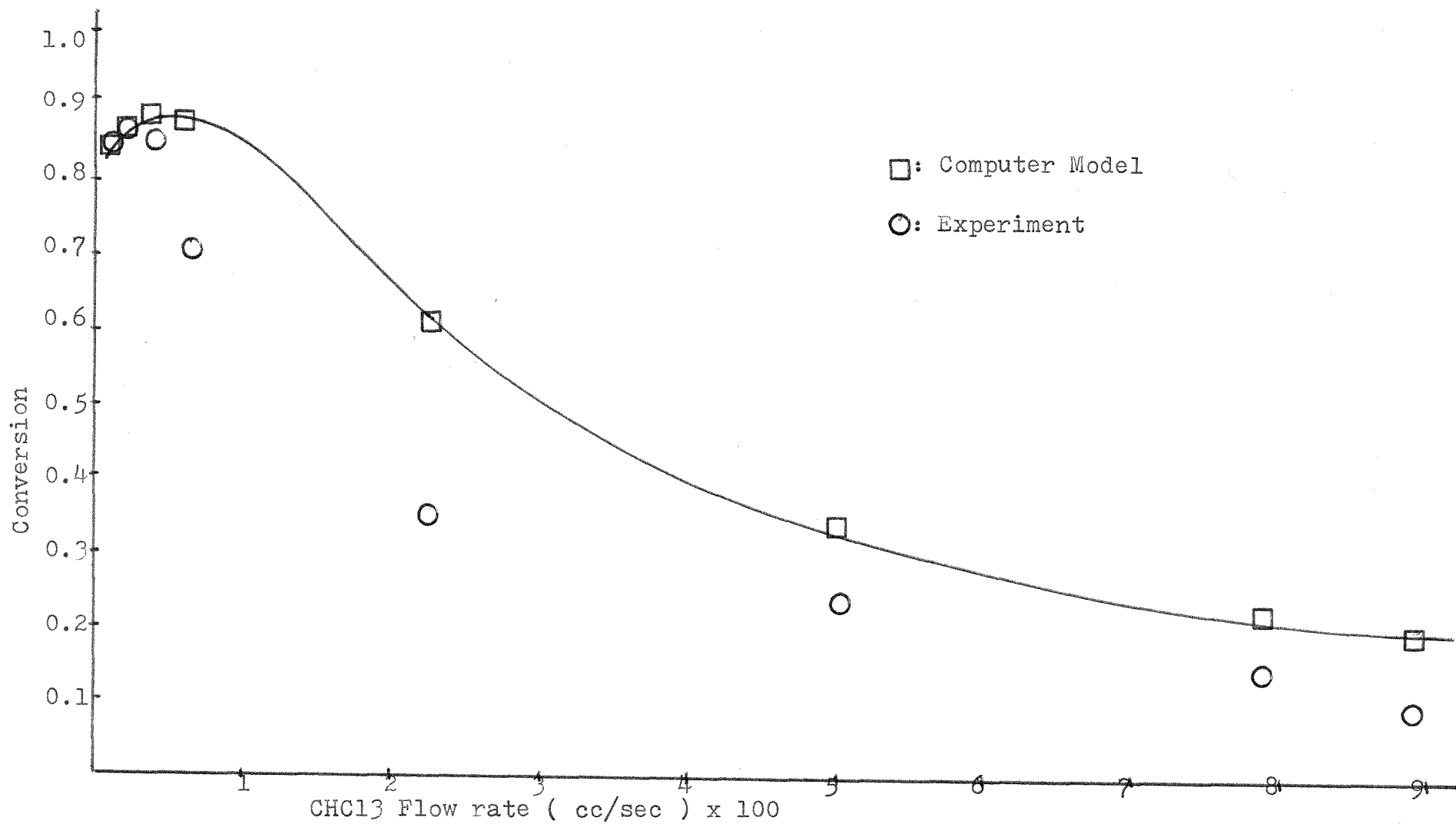


Figure 13. H-CHCl₃ Experimental and Computer Model Curves at 0.14 cc/sec(H₂).

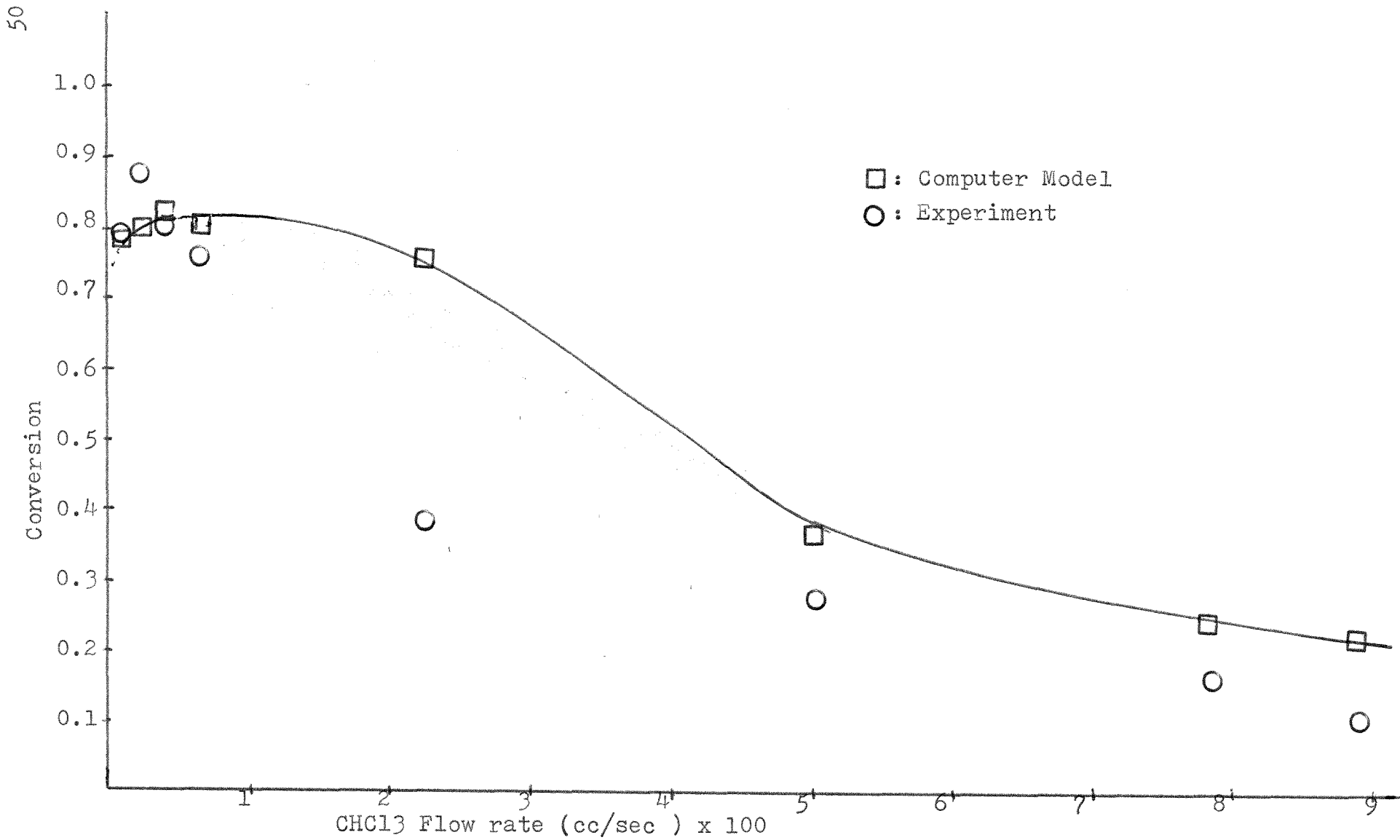


Figure 14. H-CHCl₃ Experimental and Computer Model Curves at 0.4 cc/sec (H₂).

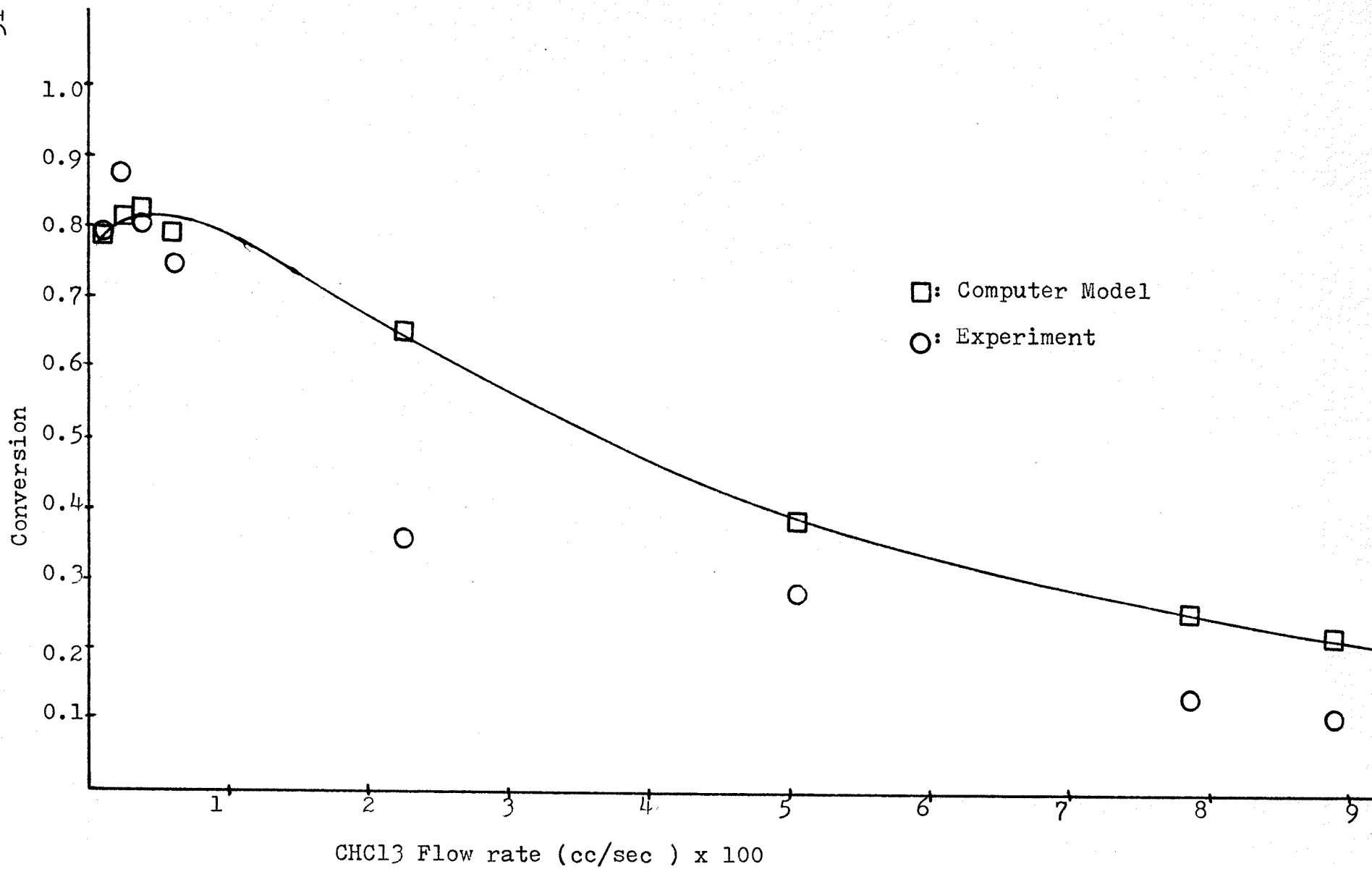


Figure 15. H-CHCl₃ Experimental and Computer Model Curves at 0.62 cc/sec (H₂).

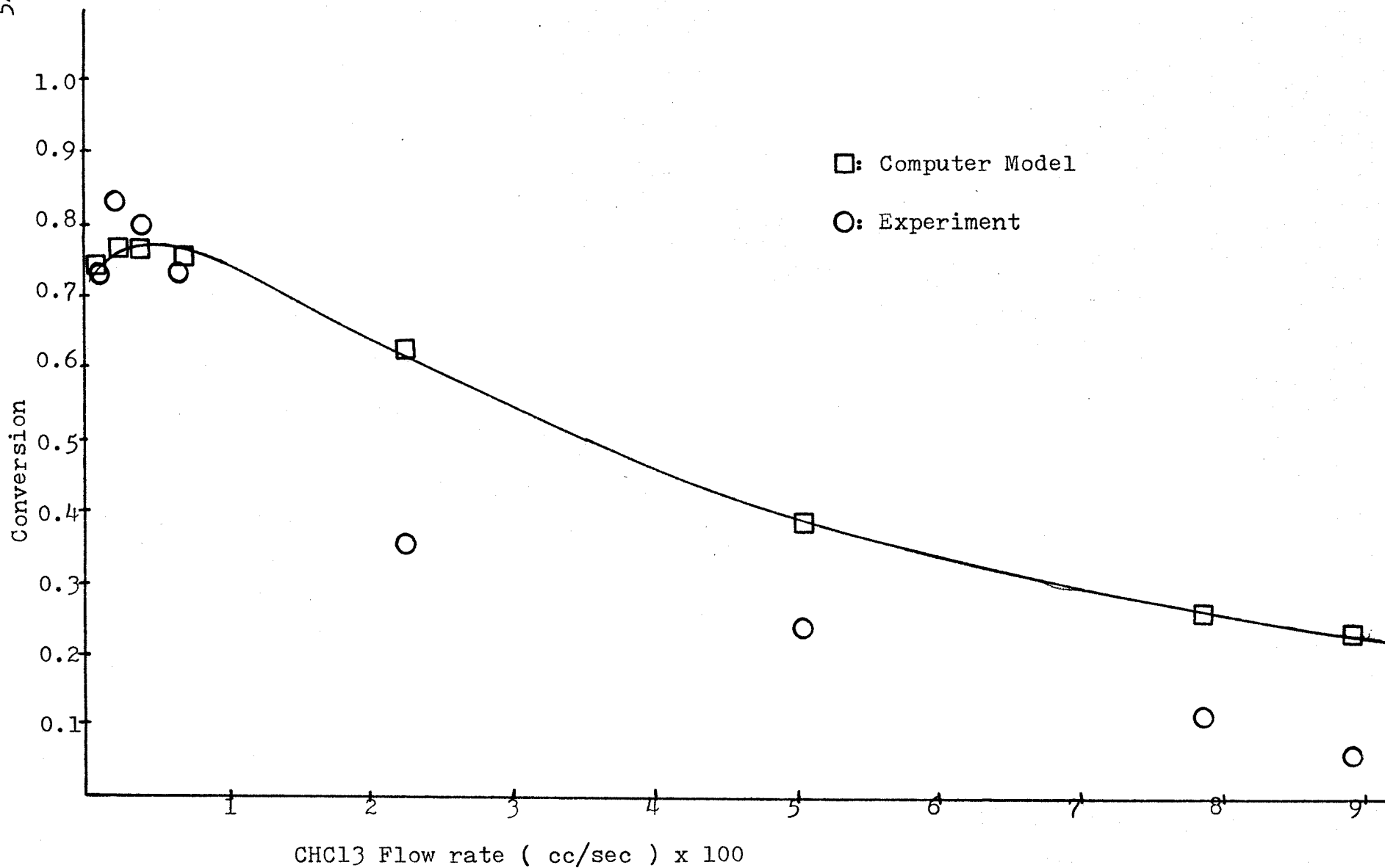


Figure 16. H-CHCl₃ Experimental and Computer Model Curves at 0.82 cc/sec (H₂).

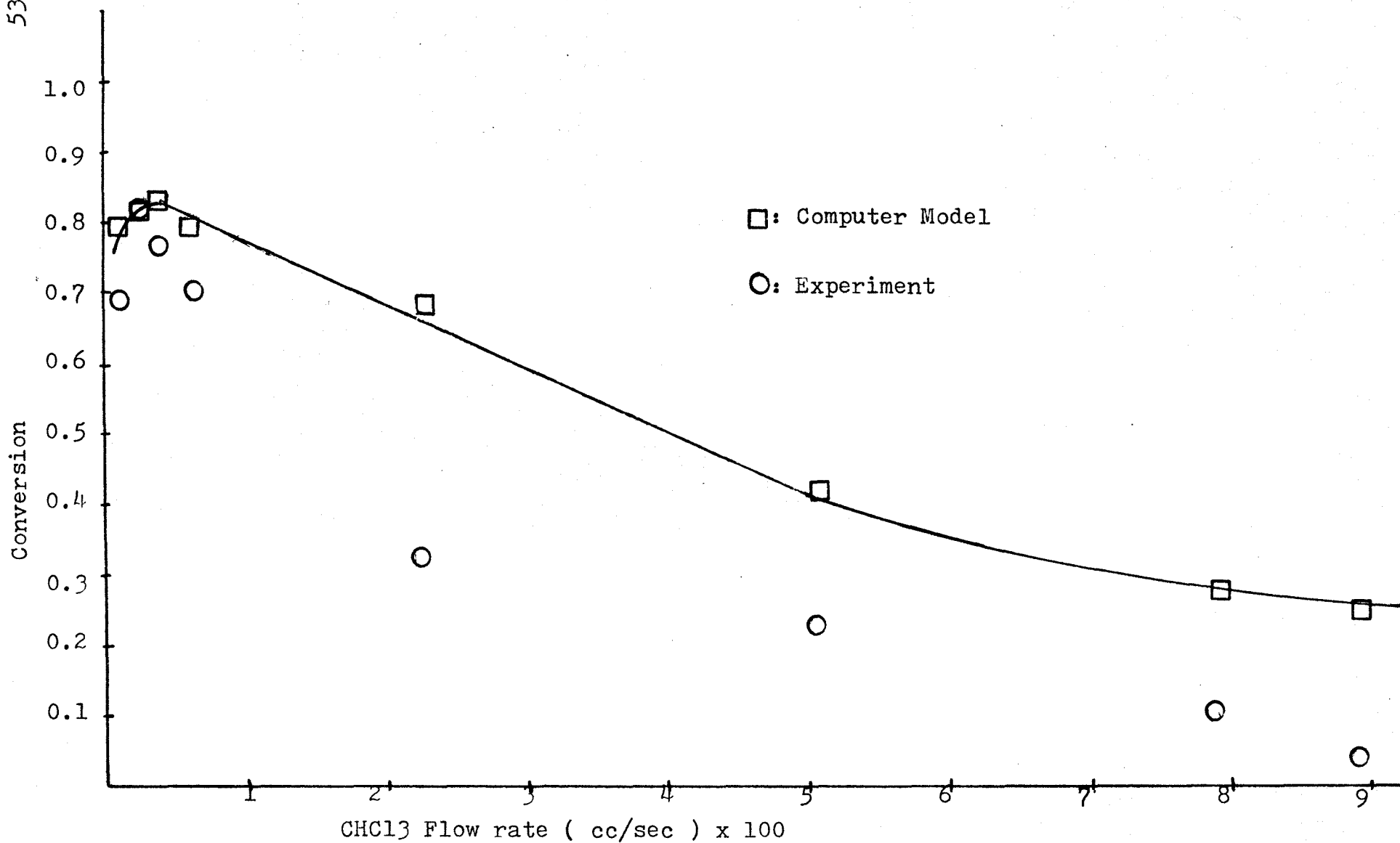


Figure 17. H-CHCl₃ Experimental and Computer Model Curves at 1.1 cc/sec (H₂).

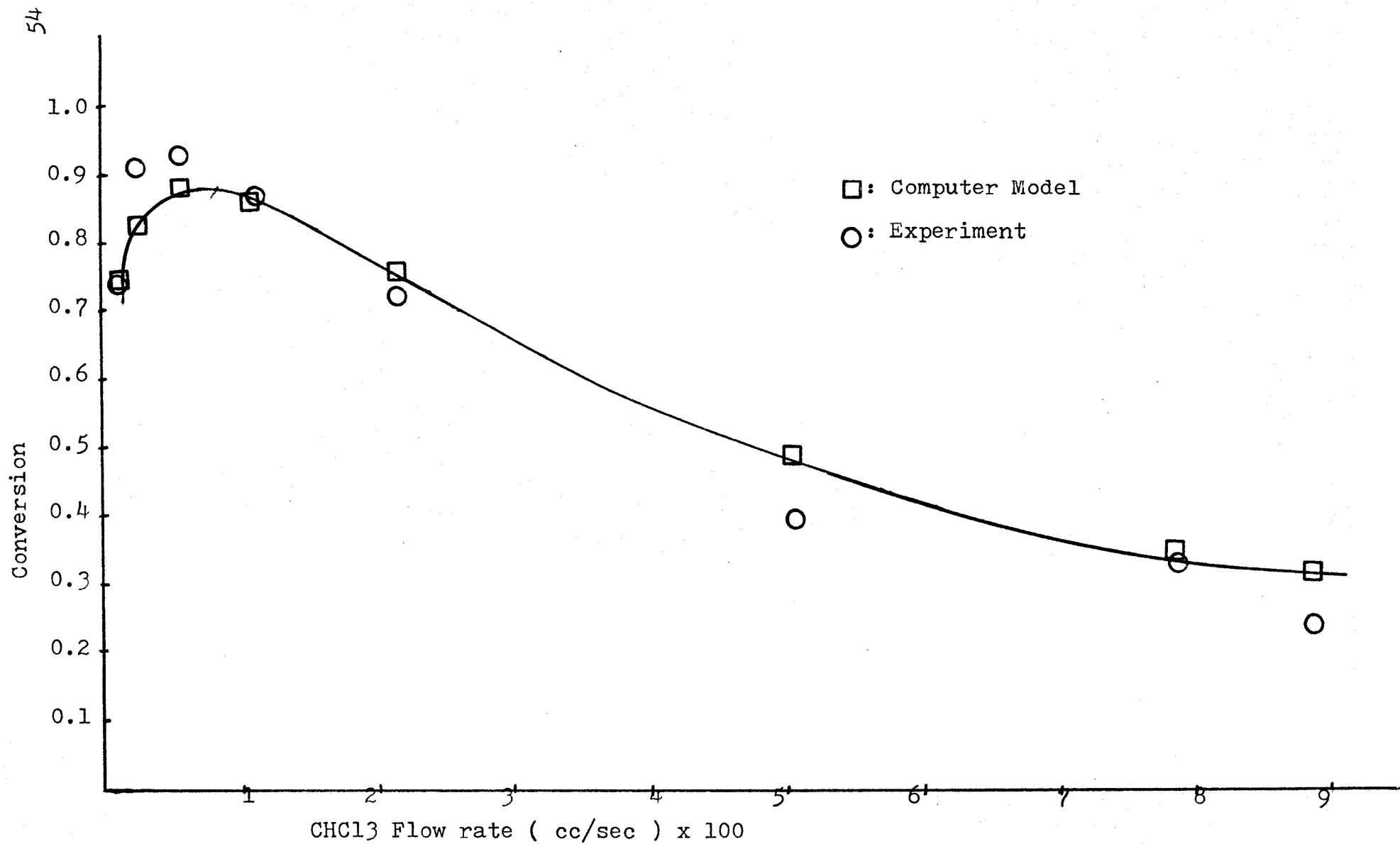


Figure 18. H-CHCl₃ Experimental and Computer Model Curves at 0.028 sec (Reaction Time).

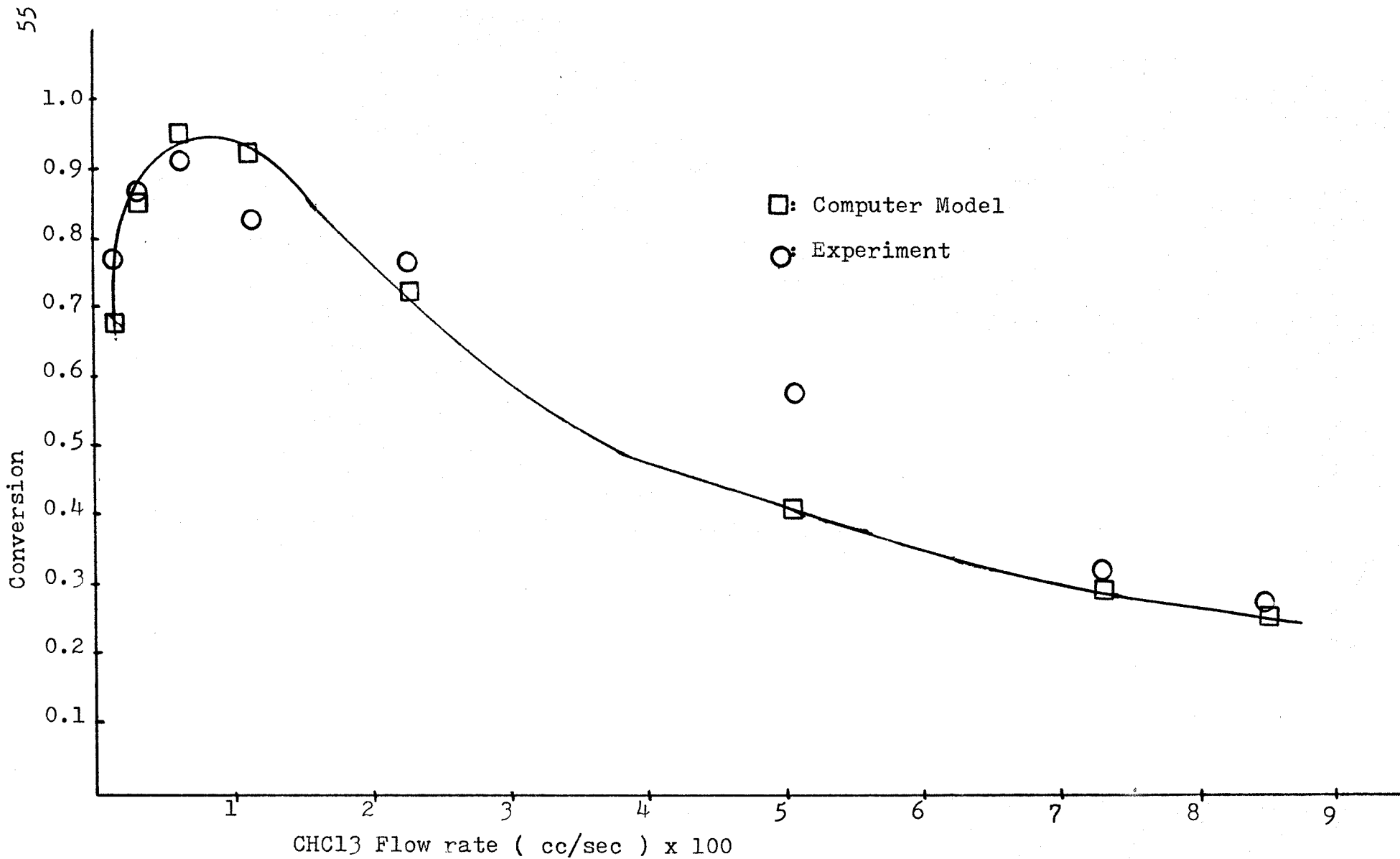


Figure 19. H- CHCl₃ Experimental and Computer Model Curves at 0.072 sec (Reaction Time).

constant for the $H-CCl_3$ reaction, is $(2.19 \pm 0.31) \times 10^{-13}$ cc/molecule-sec with 14% error in these experiments. This rate constant, however, is higher by a factor of 100 than recorded by Chari (23) 4.5×10^{-15} cc/molecule-sec. The initial concentration of chloroform used in Chari's study (23) was ten times more than that of this study. Since more chloroform concentration was present in Chari's study. This $CHCl_3$ efficiently quenched the reaction flame and maintained a lower (near room) reaction temperature. It can be thought that the reaction of hydrogen atom with chloroform, at lower chloroform concentrations, was accelerated by the flame (higher reaction temperature) due to less quenching and therefore, the rate constant is higher than that of Chari's (23).

To further elucidate an accurate room temperature reaction rate constant, two more experiments were done using the reactor which had smaller diameter and 6-port Hamiltonian injection valve instead of 4-port Hamiltonian injection valve. As shown in Figures 16 and 17, more desirable results were obtained between computer model and experimental results for the high flow velocity. It is also thought that more efficient sampling and injection system resulted in using 6-port Hamiltonian injection valve instead of 4-port valve. In the first experiment, the conversion curve from computer model well approached the experimental value and it gave k_{27} , 8.1×10^{-14} cc/mol sec. Comparing this value with earlier k_{27} obtained from larger-diameter reactor showed k_{27} was now about 40 times smaller than previous results. This means that the reaction was slower than

that previously measured. This result can be explained from the points of flow velocity. In the smaller-diameter reactor, the flow velocity was approximately three times faster than that in large reactor. Since faster flow presents more efficient mixing, dilution and more quenching of excited radicals occurred before reaction, the temperature in the reactor is, therefore, lower for the reacting species (room temperature) .

This study was performed at a reaction time of 0.028 sec. and the conversion profile of this experiment is shown in Figure 18. To test the model at another longer reaction time, the halomethane injector tube was adjusted up so that the reaction time was 2.5 times greater or 0.072 sec. The computer program was modified to take the new reaction time 0.072 seconds into account. The conversion profile of this experiment is shown along with the data of the computer model in Figure 19 and it gave the value of $3.8 * 10^{-15}$ cc/molecule-sec for k_{27} as rate constant of primary reaction . As shown in Figure 18 and Figure 19, the experimental data at 0.028 sec reaction time approached to the computer model only slightly better than that at 0.072 sec reaction time. The deviations of computer model from experimental curve were 9% and 12% for 0.028 and 0.072 sec, respectively. The rate constant of primary reaction was $8.1 * 10^{-14}$ cc/molecule-sec for 0.028 second reaction time with 9% deviation and was $3.8 * 10^{-15}$ cc/molecule-sec for 0.072 second with 12% deviation . Since the conversion curves of the model and the experiment match to a reasonably high degree with 9% and 12% deviation in both reaction times, respectively, we average these experimental values

and the rate constant is $4.2 * 10^{-14}$ cc/molecule-sec (an average value of $8.1 * 10^{-14}$ cc/molecule-sec and $3.8 * 10^{-15}$ cc/molecule-sec). It is felt that the value of $4.2 * 10^{-14}$ cc/molecule-sec for k27 is within experimental errors of 25%. The value of $4.2 * 10^{-14}$ cc/molecule-sec is slightly larger than that determined for the same reaction in the only previous study unpublished(23).

V. CONCLUSIONS

The study of mechanisms and kinetics of the reactions of atomic hydrogen with chloroform were studied in a tubular flow reactor at pressure of 2.22 to 2.82 mmHg and room temperature using a spectrometer and a gas chromatograph. Hydrogen atoms were generated by a microwave discharge, and their concentrations measured by titration with nitrogen dioxide.

The reaction flame observed is due to the strong C_2 and CH emission (8,10). Janson (37) has claimed that the C_2 swan bands observed by Gayden and Wolfhand (8) in $CCl_4 - H$ atom, $CHCl_3 - H$ atom, and $CHBr_3 - H$ atom flames were due to oxygen atoms originating from water vapor present in the hydrogen. In Arnold et. al.'s experiments the hydrogen - helium mixture was passed through three liquid nitrogen traps prior to passing through the microwave discharge. Contrary to Janson's observations in a similar experiment, C_2 emission was observed in all three systems. It was not observed however, when the hydrogen atoms were replaced by oxygen atoms. Additionally, in our experiment the hydrogen-argon mixture was passed through oxygen, water vapor and organic purification traps, using liquid nitrogen. The traps did not affect or decrease the reaction flame intensity, in agreement with Arnold's experiments.

Comparing the experimental data with those from computer model, a mechanism is suggested in the present study and is shown to be reasonable.

From the experimental results, high conversion, up to 90% of chloroform at low pressure and room temperature, means that the chloroform is a good flame inhibitor; it reduces the burning velocities of hydrocarbon/air flames. In addition, since many halomethanes are known or suspected to be carcinogenic, and since the principal products of our observed H + Halocarbon reactions are methane and an acid, HCl, the reaction over all mechanism can be applied for the destruction of toxic halocarbons, with simultaneous production of fuel (CH₄).

The nearly exclusive production of methane suggests that secondary reactions are fast and that all chloroform consumed goes toward the formation of methane with the primary reaction. The kinetic rate constant for the primary reaction of atomic hydrogen with chloroform was 4.2×10^{-14} cc/mol sec at 2980K.

There is scope for improvement in the methane collection efficiency of the sampling loop. The amount of methane trapped can be increased by modifications of the loop and flow through measurement. Detection of halocarbons can be improved via use of a more sensitive ECD detector. It is also strongly suggested for further reactions that a very small thermocouple be placed in the reactor tube to see the effects of flame quenching due to the variation of the chloroform concentration. The mixing in tube reaction zone has been improved substantially by the modifications made in the halomethane injection system during the H-CHCl₃ system. The apparatus can then be used for various other halocarbons, and rate constants determined for reactions

which have not yet been studied kinetically.

Since the study of the reactions of halomethanes with hydrogen atom can provide much needed kinetic parameters and reaction product information which are important to understanding of the chemistry of these species in incineration and in the atmosphere, it is hoped that the present study will make future studies on similar reactions simpler and yet more fruitful, in particular, considering the effects of flame quenching due to the variation of the chloroform concentration.

APPENDIX 1. Fraction of NO2 and N2O4

```
*****
1.     THIS PROGRAM IS TO FIGURE OUT THE CHANGE OF NO2 AND
2.     N2O4 FRACTION AS THE TOTAL PRESSURE DFCREASES.
3.     *****

4.     NOMENCLATURE;

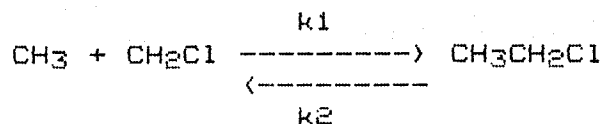
       PT IS TOTAL PRESSURE. PNOT IS PRESSURE OF NO2+N2O4.
       PNO IS PRESSURE OF NO2. PNOX IS PRESSURE OF N2O4.
       FRANO2 IS THE FRACTION OF NO2. FRANOX IS THE
       FRACTION OF N2O4. FRAAR IS THE FRACTION OF AR.

5.     PT=2.04
6.     PNOT=0.3316
7.     DKP=0.1134
8.     FRANO2=0
9.     WRITE(2,100)
10. 10  FRANO1=FRANO2
11.     PNO=(SQRT((DKP**2)+4.0*DKP*PNOT)-DKP)/2.0
12.     PNOX=PNOT-PNO
13.     FRANO2=PNO/PNOT
14.     FRANOX=1.0-FRANO2
15.     FRANOT=PNOT/PT
16.     FRAAR=1.0-FRANOT
17.     WRITE(2,200) PT,PNOT,DKP,PNO,PNOX,FRANO2,FRANOX,
18.     +FRANOT,FRAAR
19. 100  FORMAT(' ',1X,'PT',5X,'PNOT',3X,'DKP',4X,'PNO',
20.     +4X,'PNOX',3X,'FRANO2',1X,'FRANOX',1X,'FRANOT',
```

```
21.      +1X, 'FRAAR')
22. 200  FORMAT(' ',9F7.4)
23.      PNOT=(PT-0.1316)*PNOT/PT
24.      PT=(PT-0.1316)
25.      IF (PT.GT.1.84) GOTO 10
26.      COMP=(FRAN02-FRAN01)*PNOT
27.      PT=PT+COMP
28.      PNOT=PNOT+COMP
29.      IF (PT.GT.0.395) GOTO 10
30.      STOP
31.      END
```

APPENDIX 2. ESTIMATION OF RATE CONSTANT UNKNOWN BY BENSON'S
METHOD

EXAMPLE



$$\begin{aligned} \text{DEL-H}_{298} &= H(\text{CH}_3\text{Cl}) - H(\text{CH}_3) - H(\text{CH}_2\text{Cl}) \\ &= -26.7 - 35.1 - 31.1 = -92.9 \text{ Kcal/mol} \end{aligned}$$

$$\begin{aligned} \text{DEL-S}_{298} &= S(\text{CH}_3\text{CH}_2\text{Cl}) - S(\text{CH}_3) - S(\text{CH}_2\text{Cl}) \\ &= 66.1 - 46.4 - 59.6 = -39.9 \text{ cal/mol} \end{aligned}$$

$$\begin{aligned} \text{DEL-G}_{298} &= \text{DEL-H}_{298} - T * \text{DEL-S}_{298} \\ &= -92900 - 298 * (-39.9) = -81009.8 \text{ cal/mol} \end{aligned}$$

$$\begin{aligned} \text{Ln}(K_p) &= - \text{DEL-G}/RT \\ &= - (-81009.8 / (1.987 * 298)) \end{aligned}$$

Therefore,

$$K_p = 2.61 * 10^{59}$$

$$\text{And } k_1 = k_0 * \text{Exp}(-E_a/RT)$$

$$= 8.35 * 10^{-14} \text{ cc/molecule-sec}$$

$$k_2 = k_1/K_p = 8.35 * 10^{-14} / 2.61 * 10^{59}$$

$$= 3.2 * 10^{-73} \text{ cc/molecule-sec}$$

Appendix 3. Reactions

Reaction	Rate Constant	Ref.
$H+CHCl \rightarrow HCl+CHCl_2$	$k_1 = ?$	
$H+HCl \rightarrow H_2+Cl$ (-----)	$k_2 = 5.0 \times 10^{-14}$ $k(-2) = 1.6 \times 10^{-14}$	31 31
$Cl+CHCl_3 \rightarrow CCl_3+HCl$	$k_3 = 1.24 \times 10^{-13}$	28
$H+CCl_3 \rightarrow CCl_3^* \rightarrow HCl+CCl_2$ (----)	$k_4 = 1.0 \times 10^{-11}$	33
$H+CCl_2 \rightarrow CCl+HCl$	$k_5 = 1.0 \times 10^{-11}$	33
$H+CCl \rightarrow C+HCl$	$k_6 = 1.0 \times 10^{-11}$	33
$H+CHCl_2 \rightarrow CHCl+HCl$	$k_7 = 1.0 \times 10^{-11}$	33
$H+CHCl \rightarrow CH+HCl$	$k_8 = 1.0 \times 10^{-11}$	33
$H+C+M \rightarrow CH+M$	$k_9 = 2.41 \times 10^{-13}$	35
$H+CH+M \rightarrow CH_2+M$	$k_{10} = 2.41 \times 10^{-13}$	35
$H+CH_2+M \rightarrow CH_3+M$	$k_{11} = 2.41 \times 10^{-13}$	35
$H+CH_3+M \rightarrow CH_4+M$	$k_{12} = 2.41 \times 10^{-13}$	35
$Cl+CH_4 \rightarrow CH_3+HCl$ (-----)	$k_{13} = 1.25 \times 10^{-13}$ $k(-13) = 1.18 \times 10^{-13}$	32 36
$Cl+CH_3 \rightarrow CH_3Cl$	$k_{14} = 1.72 \times 10^{-12}$	36
$Cl+CH_3Cl \rightarrow HCl+CH_2Cl$ (-----)	$k_{15} = 2.8 \times 10^{-13}$ $k(-15) = 2.51 \times 10^{-13}$	36 36
$CH_3+CH_3 \rightarrow C_2H_6$	$k_{16} = 4.18 \times 10^{-14}$	36
$CH_3+CH_2Cl \rightarrow CH_3CH_2Cl$	$k_{17} = 8.35 \times 10^{-14}$	36
$CH_2Cl+CH_2Cl \rightarrow ClCH_2CH_2Cl$	$k_{18} = 1.6 \times 10^{-14}$	36
$H+H+M \rightarrow H_2+M$	$k_{19} = 1.54 \times 10^{-15}$	35

APPENDIX 4. Calculation of hydrogen atom and chloroform concentrations

$$(1). F_t = F_{Ar} + F_{H_2} + F_{CHCl_3} \\ = 18.87 + 0.16 + (\text{very small}) = 19.03 \text{ cc/sec}$$

$$(2). \text{Pressure of Reactor} = 3.15 * 0.959 / 1.36 \\ = 2.22 \text{ mmHg}$$

$$(3). \text{Total flow at 2.22 mmHg} = 19.03 * 760 / 2.22 \\ = 6514.77 \text{ cc/sec}$$

Molecules of total flow

$$= 6514.77 * (2.22/760) * 6 * 10^{23} / (82.06 * 298) \\ = 4.67 * 10^{20} \text{ molecules/sec}$$

and

$$\# \text{ molecules/cc} = 4.67 * 10^{20} / 6514.77 \\ = 7.17 * 10^{16} \text{ molecules/cc}$$

$$(4). \text{Fraction of [H]} \\ = \text{NO}_2 \text{ flow (extrapolated) / total flow} \\ = 0.43 * (0.073 + 2 * 0.08) / 19.03 \\ = 5.3 * 10^{-3}$$

Hydrogen atoms

$$= 5.3 * 10^{-3} * 7.17 * 10^{16} \\ = 3.8 * 10^{14} \text{ molecules/cc}$$

(5). Fraction of hydrogen

$$= F_{H_2} / F_t \\ = 0.16 / 19.03 \\ = 0.00841$$

(6). % dissociation

$$= \# \text{ of H} / \# \text{ of H}$$

$$= 3.8 * 10^{14} * 100 / ((6.03 * 10^{14}) * 2)$$

$$= 31.5 \%$$

(7). Reaction time at 35 cm distance

$$= \text{Distance} / \text{Flow Velocity}$$

$$= 35 / (6514.77 / 5.31)$$

$$= 0.028 \text{ sec.}$$

APPENDIX 5. Computer model

```

1. *****
2. MOSTLY POSSIBLE MECHANISM WAS POSTURATED AND THE
3. KINETICS SIMULATED ON AN UNIVAC 90/80-3 COMPUTER
4. BY SOLVING THE SIMULTANEOUS FIRST-ORDER DIFFERENTIAL
5. EQUATIONS DESCRIBING THE TIME DEPENDENCE OF THE
6. CONCENTRATION OF THE VARIOUS CHEMICAL SPECIES,
7. USING BOTH RUNGE-KUTTA FORTH INTEGRATION METHOD
8. AND ROSENBROCK OPTIMIZATION METHOD
9. *****

10. NOMENCLATURE
    ALL K'S ARE RATE CONSTANTS.
    RTM IS REACTION TIME.
    T IS TIME INTERVAL FOR EACH ITERATION.
    EACH UNIT OF H, C, C1, HCl, CC13H, CC12H, CC1H, CH, CH2, CH3,
    CH4, H2 IS MOLECULES/CC OR ATOMS/CC.
    H0, H2O, AND CC13H0 ARE CONCENTRATION AT ZERO TIME.

11. MAIN LINE PROGRAM FOR ROSENBROCK HILLCLIMB
12. -----

13. DIMENSION X(8), E(8), V(8,8), SA(8), D(8), H(8), AL(8),
14. PH(8), A(8,8), B(8,8), BX(8), DA(8), VV(8,8), EINT(8),
15. VM(8)
16. DIMENSION Y(8,20), G(8,20), ELM(8,23), Z(8,1)
17. DOUBLE PRECISION Y, G, X, DK2, RDK2, DK3, DK4, DK5, DK6, DK7
18. DOUBLE PRECISION DK8, DK9, DK10, DK11, DK12, DK13, RDK13
19. DOUBLE PRECISION DK14, DK15, RDK15, DK16, DK17, DK18, DK19
20. DOUBLE PRECISION DK20, HD, T, TMAX, ELM, Z
21. INTEGER RUNGE
22. COMMON KOUNT
23. INTEGER P
24. INTEGER PR
25. INTEGER R
26. INTEGER C
27. REAL LC
28. DATA M, P, L, LOOPY, PR, ND, NDATA, NSTEP/-1, 1, 1, 10, 1, 0, 0, 0/
29. X(1)=4.5D-14
30. E(1)=1.0E-15
31. WRITE(6, 13)
32. 13   FORMAT(/, 10X, 'ROSENBROCK HILLCLIMB PROCEDURE')
33.     IF(ND-1) 30, 20, 30
34. 20   DO 300 KA=1, NDATA
35.     READ (NI, 2) DA(KA)
36.     2   FORMAT(1E10.4)
37. 300   CONTINUE
38. 30   LAP=PR-1
39.     LOOP=0
40.     ISW=0
41.     INIT=0

```



```

42.      KOUNT=0
43.      TERM=0.0
44.      DELY=1.0E-2
45.      F1=0.0
46.      NPAR=NDATA
47.      N=L
48.      DO 40 K=1,L
49.  40      AL(K)=(CH(X,DA,N,NPAR,K)-CG(X,DA,N,NPAR,K))*0.0001
50.      DO 60 I=1,P
51.      DO 60 J=1,P
52.      V(1,J)=0.0
53.      IF (I-J) 60,61,60
54.  61      V(I,J)=1.0
55.  60      CONTINUE
56.      DO 65 KK=1,P
57.      EINT(KK)=E(KK)
58.  65      CONTINUE
59.  1000    DO 70 J=1,P
60.      IF (NSTEP.EQ.0) E(J)=EINT(J)
61.      SA(J)=2.0
62.  70      D(J)=0.0
63.      FBEST=F1
64.  80      I=1
65.      IF(INIT.EQ.0) GOTO 120
66.  90      DO 110 K=1,P
67.  110     X(K)=X(K)+E(I)*V(I,K)
68.      DO 50 K=1,L
69.  50      H(K)=F0
70.  120     F1=F(X,N)
71.      F1=M*F1
72.      IF(ISW.EQ.0) F0=F1
73.      ISW=1
74.      IF(ABS(FBEST-F1)-DELY) 122,122,125
75.  122     TERM+1.0
76.      GOTO 450
77.  125     CONTINUE
78.      J=1
79.  130     XC=CX(X,DA,N,NPAR,J)
80.      LC=CG(X,DA,N,NPAR,J)
81.      UC=CH(X,DA,N,NPAR,J)
82.      IF(XC.LE.LC) GOTO 420
83.      IF(XC.GE.UC) GOTO 420
84.      IF(F1.LT.F0) GOTO 420
85.      IF(XC.LT.LC+AL(J)) GOTO 140
86.      IF(XC.GT.UC-AL(J)) GOTO 140
87.      H(J)=F0
88.      GOTO 210
89.  140     CONTINUE
90.      BW=AL(J)
91.      IF(XC.LE.LC.OR.UC.LE.XC) GOTO 150
92.      IF(LC.LT.XC.AND.XC.LT.LC+BW) GOTO 160
93.      IF(UC-BW.LT.XC.AND.XC.LT.UC) GOTO 170
94.      PH(J)=1.0
95.      GOTO 210

```

```

96. 150 PH(J)=0.0
97. GOTO 190
98. 160 PW=(LC+BW-XC)/BW
99. GOTO 180
100. 170 PW=(XC-UC+BW)/BW
101. 180 PH(J)=1.0-(3.0*PW)+(4.0*PW*PW)-(2.0*PW*PW*PW)
102. 190 F1=H(J)+(F1-H(J))*PH(J)
103. 210 CONTINUE
104. 220 INIT=1
105. IF(F1.LT.F0) GOTO 420
106. D(I)=D(I)+E(I)
107. E(I)=3.0*E(I)
108. F0=F1
109. IF(SA(I).GE.1.5) SA(I)=1.0
110. 230 DO 240 JJ=1,P
111. IF(SA(JJ).GE.0.5) GOTO 440
112. 240 CONTINUE
113. LOOP=LOOP+1
114. LAP=LAP+1
115. IF(LAP.EQ.PR) GOTO 450
116. GOTO 1000
117. 420 IF(INIT.EQ.0) GOTO 450
118. DO 430 IX=1,P
119. 430 X(IX)=X(IX)-E(I)*V(I,IX)
120. E(I)=-0.5*E(I)
121. IF(SA(I).LT.1.5) SA(I)=0.0
122. GOTO 230
123. 440 CONTINUE
124. GOTO 80
125. 450 WRITE(6,3)
126. 3 FORMAT(//,2X,5HSTAGE,8X,8HFUNCTION)
127. WRITE(6,4) LOOP,F0
128. 4 FORMAT(1H,15,E20.8)
129. WRITE(6,14) KOUNT
130. 14 FORMAT(/,2X,'NUMBER OF FUNCTION EVALUATIONS= ',I8)
131. WRITE(6,5)
132. 5 FORMAT(/,2X,25HVALUES OF X AT THIS STAGE)
133. WRITE(6,6) (JM,X(JM),JM=1,P)
134. 6 FORMAT(/,2X,2HX(,I2,4H) = ,1PE14.6)
135. LAP=0
136. IF(INIT.EQ.0) GOTO 470
137. IF(TERM.EQ.1.0) GOTO 480
138. IF(LOOP.GE.LOOPY) GOTO 480
139. GOTO 1000
140. 470 WRITE(6,7)
141. 7 FORMAT(///,2X,'THE START POINT MUST NOT VIOLATE')
142. 480 CONTINUE
143. WRITE(6,11)
144. 11 FORMAT(//,2X,16HFINAL STEP SIZES)
145. WRITE(6,12) (J,E(J),J=1,P)
146. 12 FORMAT(/,2X,2HS(,I1,4H) = ,F10.8)

```

```

*****
THIS IS A COMPUTER MODEL FOR KINETICS OF H-CHCL3
REACTION, COMBINING RUNGE-KUTTA (FORTH) METHOD FOR
DIFFERENTIATION OF THE RATE EQUATIONS WITH ROSEN BROCK
METHOD FOR OPTIMIZATION OF THE SYSTEM.
*****

```

```

147.      T1=0.0
148.      HD=2.0D-4
149.      TMAX1=0.02831
150.      TMAX2=0.02849
151.      DO 1500 MM=1,8
152.      T=0.0
153.      DO 2000 L=1,20
164.      Y(MM,L)=0.0
165.      IF(L.EQ.1) Y(MM,1)=3.8D14
166.      IF(L.EQ.5) Y(MM,5)=6.03D14
167.      G(MM,L)=0.0
168. 2000  CONTINUE
169.      DO 3000 I=1,22
170.      ELM(MM,I)=0.0
171. 3000  CONTINUE
172.      Y(1,2)=3.39D12
173.      Y(2,2)=8.36D12
174.      Y(3,2)=2.12D13
175.      Y(4,2)=4.26D13
176.      Y(5,2)=8.14D13
177.      Y(6,2)=1.92D14
178.      Y(7,2)=2.98D14
179.      Y(8,2)=3.35D14
180.      DO 2500 J=1,8
181.      Z(J,1)=Y(MM,2)
182. 2500  CONTINUE
183.      WRITE(6,444) T1
184.      WRITE(6,222)
185.      WRITE(6,707) Y(MM,1),Y(MM,2),Y(MM,3),Y(MM,5)
186.      WRITE(6,333)
187.      WRITE(6,707) Y(MM,7),Y(MM,9),Y(MM,10),Y(MM,15)
188. 520   N1=RUNGE(MM,20,Y,G,T,HD)
189.      N2=RATE(MM,ELM,X,Y)
190.      IF(N1.NE.1) GOTO 540
191.      G(MM,1)=-ELM(MM,1)-ELM(MM,2)+ELM(MM,3)-ELM(MM,5)-
192.      ELM(MM,6)-ELM(MM,7)-ELM(MM,8)-ELM(MM,9)-ELM(MM,10)
193.      -ELM(MM,11)-ELM(MM,12)-ELM(MM,13)-
194.      ELM(MM,22)*2.0-ELM(MM,23)
195.      G(MM,2)=-ELM(MM,1)-ELM(MM,4)-ELM(MM,23)
196.      G(MM,3)=ELM(MM,1)-ELM(MM,2)+ELM(MM,3)+ELM(MM,4)+
197.      ELM(MM,5)+ELM(MM,6)+ELM(MM,7)+ELM(MM,8)+ELM(MM,9)
198.      +ELM(MM,14)-ELM(MM,15)+ELM(MM,17)-ELM(MM,18)
199.      G(MM,4)=ELM(MM,1)-ELM(MM,8)
200.      G(MM,5)=ELM(MM,2)-ELM(MM,3)+ELM(MM,22)+ELM(MM,23)
201.      G(MM,6)=ELM(MM,2)-ELM(MM,3)-ELM(MM,4)-ELM(MM,14)+
202.      ELM(MM,15)-ELM(MM,17)+ELM(MM,18)-ELM(MM,16)

```

```

203.      G(MM, 7)=ELM(MM, 4)-ELM(MM, 5)+ELM(MM, 23)
204.      G(MM, 8)=ELM(MM, 5)-ELM(MM, 6)
205.      G(MM, 9)=ELM(MM, 6)-ELM(MM, 7)
206.      G(MM, 10)=ELM(MM, 7)-ELM(MM, 10)
207.      G(MM, 11)=ELM(MM, 8)-ELM(MM, 9)
208.      G(MM, 12)=ELM(MM, 10)-ELM(MM, 11)
209.      G(MM, 13)=ELM(MM, 11)-ELM(MM, 12)
210.      G(MM, 14)=ELM(MM, 12)-ELM(MM, 13)+ELM(MM, 14)-ELM(MM, 15)-
211.      ELM(MM, 16)-2.0*ELM(MM, 19)-ELM(MM, 20)
212.      G(MM, 15)=ELM(MM, 13)-ELM(MM, 14)+ELM(MM, 15)
213.      G(MM, 16)=ELM(MM, 16)-ELM(MM, 17)+ELM(MM, 18)
214.      G(MM, 17)=ELM(MM, 17)-ELM(MM, 18)-ELM(MM, 20)
215.      -2.0*ELM(MM, 21)
216.      G(MM, 18)=ELM(MM, 19)
217.      G(MM, 19)=ELM(MM, 20)
218.      G(MM, 20)=ELM(MM, 21)
219.      GOTO 520
220. 540      IF(T.GE.TMAX1.AND.T.LE.TMAX2) GOTO 31
221.      GOTO 52
222. 31      J=MM
223.      CONV=1.0-Y(MM, 2)/Z(J, 1)
224.      WRITE(6, 606) T
225.      WRITE(6, 222)
226.      WRITE(6, 707) Y(MM, 1), Y(MM, 2), Y(MM, 3), Y(MM, 5)
227.      WRITE(6, 333)
228.      WRITE(6, 707) Y(MM, 7), Y(MM, 9), Y(MM, 10), Y(MM, 15)
229.      WRITE(6, 555) CONV
230. 1500     CONTINUE
231. 222      FORMAT(' ', 2X, 'H', 17X, 'CCL3H', 13X, 'HCL', 15X, 'H2')
232. 333      FORMAT(' ', 2X, 'CL', 16X, 'CCL3', 14X, 'CA', 16X, 'CH4')
233. 555      FORMAT(' ', 2X, 'CONVERSION=', 7X, E13.7)
234. 444      FORMAT(/, 3X, 'INITIAL TIME=', 4X, F7.5)
235. 606      FORMAT(' ', 2X, 'FINAL TIME=', 6X, F7.5)
236. 707      FORMAT(' ', 2X, E13.7, 3(5X, E13.7))
237.      STOP
238.      END

```

THIS FUNCTION, F(X,N), IS MINIMIZED BY ROSENBROCK
HILLCLIMB OPTIMIZATION METHOD.
THIS IS OBJECTIVE FUNCTION.

```

239.      FUNCTION F(X,N)
240.      DOUBLE PRECISION Y, G, X, DK2, RDK2, DK3, DK4, DK5, DK6, DK7
241.      DOUBLE PRECISION DK8, DK9, DK10, DK11, DK12, DK13, RDK13
242.      DOUBLE PRECISION DK14, DK15, RDK15, DK16, DK17, DK18, DK19
243.      DOUBLE PRECISION DK20, HD, T, TMAX, ELM, Z, VAL
244.      COMMON KOUNT
245.      INTEGER RUNGE
246.      DIMENSION Y(8, 20), G(8, 20), ELM(MM, 22), Z(8, 1), X(8),

```

```

247. VAL(8,1)
248. T1=0.0249.
249. HD=2.0D-4
250. TMAX1=0.02831
251. TMAX2=0.02849
252. DATA(VAL(NN,1),NN=1,8)/8.5D11,5.89D11,1.62D12,
253. 5.84D12,2.35D13,1.18D14,1.94D14,2.53D14/
254. SUM=0.0
255. X1=X(1)
256. DO 1000 MM=1,8
257. T=0.0
258. DO 2000 L=1,20
259. Y(MM,L)=0.0
260. IF(L.EQ.1) Y(MM,1)=3.8D14
261. IF(L.EQ.5) Y(MM,5)=6.03D14
262. G(MM,L)=0.0
263. 2000 CONTINUE
264. DO 3000 I=1,22
265. ELM(MM,I)=0.0
266. 3000 CONTINUE
267. Y(1,2)=3.39D12
268. Y(2,2)=8.36D12
269. Y(3,2)=2.12D13
270. Y(4,2)=4.26D13
271. Y(5,2)=8.14D13
272. Y(6,2)=1.92D14
273. Y(7,2)=2.98D14
274. Y(8,2)=3.35D14
275. DO 2500 J=1,8
276. Z(J,1)=Y(MM,2)
277. 2500 CONTINUE
278. 520 N1=RUNGE(MM,20,Y,G,T,HD)
279. N2=RATE(MM,ELM,X,Y)
280. IF(N1.NE.1) GOTO 540
281. G(MM,1)=-ELM(MM,1)-ELM(MM,2)+ELM(MM,3)-ELM(MM,5)-
282. ELM(MM,6)-ELM(MM,7)-ELM(MM,8)-ELM(MM,9)-ELM(MM,10)-
283. -ELM(MM,11)-ELM(MM,12)-ELM(MM,13)-
284. ELM(MM,22)*2.0-ELM(MM,23)
285. G(MM,2)=-ELM(MM,1)-ELM(MM,4)-ELM(MM,23)
286. G(MM,3)=ELM(MM,1)-ELM(MM,2)+ELM(MM,3)+ELM(MM,4)+
287. ELM(MM,5)+ELM(MM,6)+ELM(MM,7)+ELM(MM,8)+ELM(MM,9)
288. +ELM(MM,14)-ELM(MM,15)+ELM(MM,17)-ELM(MM,18)
289. G(MM,4)=ELM(MM,1)-ELM(MM,8)
290. G(MM,5)=ELM(MM,2)-ELM(MM,3)+ELM(MM,22)+ELM(MM,23)
291. G(MM,6)=ELM(MM,2)-ELM(MM,3)-ELM(MM,4)-ELM(MM,14)+
292. ELM(MM,15)-ELM(MM,17)+ELM(MM,18)-ELM(MM,16)
293. G(MM,7)=ELM(MM,4)-ELM(MM,5)+ELM(MM,23)
294. G(MM,8)=ELM(MM,5)-ELM(MM,6)
295. G(MM,9)=ELM(MM,6)-ELM(MM,7)
296. G(MM,10)=ELM(MM,7)-ELM(MM,10)
297. G(MM,11)=ELM(MM,8)-ELM(MM,9)
298. G(MM,12)=ELM(MM,10)-ELM(MM,11)
299. G(MM,13)=ELM(MM,11)-ELM(MM,12)
300. G(MM,14)=ELM(MM,12)-ELM(MM,13)+ELM(MM,14)-ELM(MM,15)-

```

```

301.      ELM(MM, 16)=-2.0*ELM(MM, 19)-ELM(MM, 20)
302.      G(MM, 15)=ELM(MM, 13)-ELM(MM, 14)+ELM(MM, 15)
303.      G(MM, 16)=ELM(MM, 16)-ELM(MM, 17)+ELM(MM, 18)
304.      G(MM, 17)=ELM(MM, 17)-ELM(MM, 18)-ELM(MM, 20)
305.      -2.0*ELM(MM, 21)
306.      G(MM, 18)=ELM(MM, 19)
307.      G(MM, 19)=ELM(MM, 20)
308.      G(MM, 20)=ELM(MM, 21)
309.      GOTO 520
310. 540      IF(T.GE.TMAX1.AND.T.LE.TMAX2) GOTO 31
311.      GOTO 520
312. 31      EXP=VAL(MM, 1)
313.      CAL=Y(MM, 2)
314.      IF(EXP-CAL) 377, 377, 477
315. 377      DIFF=1.0-EXP/CAL
316.      GOTO 577
317. 477      DIFF=1.0-CAL/EXP
318. 577      CONTINUE
319.      SUM=SUM+DIFF
320.      F=SUM
321.      WRITE(6, 125) F, DIFF
322.      WRITE(6, 135) X1
323. 125      FORMAT(/, 2X, 'F= ', E13.6, 5X, 'ERR= ', E13.6)
324. 135      FORMAT(/, 2X, 'X1= ', E13.6)
325. 1000     CONTINUE
326.      KOUNT+KOUNT+1
327.      RETURN
328.      END

```

THE FUNCTIONS, RUNGE AND RATE, EMPLOY THE FOURTH-
ORDER RUNGE-KUTTA METHOD WITH KUTTA'S COEFFICIENTS
TO INTEGRATE A SYSTEM OF N SIMULTANEOUS FIRST ORDER
ORDINARY DIFFERENTIAL EQUATIONS $G=DK*Y*Y'$.

```

329.      FUNCTION RUNGE(MM, N, Y, G, T, H)
330.      INTEGER RUNGE
331.      DOUBLE PRECISION Y, G, T, H
332.      DIMENSION PHI(50, 100), SAVEY(50, 100), Y(8, N), G(8, N)
333.      DATA IM/0/
334.      IM=IM+1
335.      GOTO (1, 2, 3, 4, 5), IM
336. 1      RUNGE=1
337.      RETURN
338. 2      DO 22 J=1, N
339.      SAVEY(MM, J)=Y(MM, J)
340.      PHI(MM, J)=PHI(MM, J)+2.0*G(MM, J)
341. 22      Y(MM, J)=SAVEY(MM, J)+0.5*G(MM, J)
342.      T=T+0.5*H
343.      RUNGE=1

```

```

345.     RETURN
346.   3     DO 33 J=1,N
347.     PHI(MM, J)+2.0*G(MM, J)
348.   33     Y(MM, J)=SAVEY(MM, J)+0.5*H*G(MM, J)
349.     RUNGE=1
350.     RETURN
351.   4     DO 44 J=1,N
352.     PHI(MM, J)=PHI(MM, J)+2.0*G(MM, J)
353.   44     Y(MM, J)=SAVEY(MM, J)+H*G(MM, J)
354.     T=T+0.5*H
355.     RUNGE=1
356.     RETURN
357.   5     DO 55 J=1,N
358.   55     Y(MM, J)=SAVEY(MM, J)+(PHI(MM, J)+G(MM, J))*H/6.0
359.     IM=0
360.     RUNGE=0
361.     RETURN
362.     END
363.     FUNCTION RATE(M, ELM, X, Y)
364.     DOUBLE PRECISION Y, X, DK2, RDK2, DK3, DK4, DK5, DK6, DK7
365.     DOUBLE PRECISION DK8, DK9, DK10, DK11, DK12, DK13, RDK13
366.     DOUBLE PRECISION DK14, DK15, RDK15, DK16, DK17, DK18, DK19
367.     DOUBLE PRECISION DK20, ELM
368.     DIMENSION ELM(8, 23), Y(8, 20), X(8)
369.     DATA DK2, RDK2, DK3, DK4, DK5, DK6, DK7, DK8, DK9, DK10, DK11,
370.     DK12, DK13, RDK13, DK14/5.0D-14, 1.60D-14, 3.0D-11, 1.0D-11
371.     1.0D-11, 1.0D-11, 1.0D-11, 1.0D-11, 2.41D-13, 2.41D-13,
372.     2.41D-13, 2.41D-13, 1.25D-13, 1.18D-13, 1.72D-12/
373.     DATA DK15, RDK15, DK16, DK18, DK19, DK20/2.8D-13,
374.     2.51D-13, 4.18D-14, 8.35D-14, 1.87D-14, 1.54D-15/
375.     X1=X(1)
376.     RATE=0.0
377.     ELM(M, 1)=X1*Y(M, 1)*Y(M, 2)
378.     ELM(M, 2)=DK2*Y(M, 1)*Y(M, 3)
379.     ELM(M, 3)=RDK2*Y(M, 5)*Y(M, 6)
380.     ELM(M, 4)=DK3*Y(M, 6)*Y(M, 2)
381.     ELM(M, 5)=DK4*Y(M, 1)*Y(M, 7)
382.     ELM(M, 6)=DK5*Y(M, 1)*Y(M, 8)
383.     ELM(M, 7)=DK6*Y(M, 1)*Y(M, 9)
384.     ELM(M, 8)=DK7*Y(M, 1)*Y(M, 4)
385.     ELM(M, 9)=DK8*Y(M, 1)*Y(M, 11)
386.     ELM(M, 10)=DK9*Y(M, 1)*Y(M, 10)
389.     ELM(M, 11)=DK10*Y(M, 1)*Y(M, 12)
390.     ELM(M, 12)=DK11*Y(M, 1)*Y(M, 13)
391.     ELM(M, 13)=DK12*Y(M, 1)*Y(M, 14)
392.     ELM(M, 14)=DK13*Y(M, 6)*Y(M, 15)
393.     ELM(M, 15)=RDK13*Y(M, 3)*Y(M, 14)
394.     ELM(M, 16)=DK14*Y(M, 6)*Y(M, 14)
395.     ELM(M, 17)=DK15*Y(M, 6)*Y(M, 16)
396.     ELM(M, 18)=RDK15*Y(M, 3)*Y(M, 17)
397.     ELM(M, 19)=DK16*Y(M, 14)*Y(M, 14)
398.     ELM(M, 20)=DK18*Y(M, 14)*Y(M, 17)
399.     ELM(M, 21)=DK19*Y(M, 17)*Y(M, 17)
400.     ELM(M, 22)=DK20*Y(M, 1)*Y(M, 1)

```

```
401.      ELM(M, 23) = (1.0/7.2) * X1 * Y(M, 1) * Y(M, 2)
402.      RETURN
403.      END
```

FUNCTION CX SPECIFIES FUNCTION TO BE CONSTRAINED.

```
404.      FUNCTION CX (X, DA, N, NPAR, K)
405.      DOUBLE PRECISION X
406.      DIMENSION X(8), DA(8)
407.      CX = X(K)
408.      RETURN
409.      END
```

FUNCTION CG SPECIFIES LOWER BOUND OF CONSTRAINTS.

```
410.      FUNCTION CG(X, DA, N, NPAR, K)
411.      DOUBLE PRECISION X
412.      DIMENSION X(8), DA(8)
413.      CG = 1.0E-14
414.      RETURN
415.      END
```

FUNCTION CH SPECIFIES UPPER BOUND OF CONSTRAINTS.

```
416.      FUNCTION CH(X, DA, N, NPAR, K)
417.      DIMENSION X(8), DA(8)
418.      DOUBLE PRECISION X
419.      1      CH = 9.0E-14
420.      4      RETURN
421.      END
```


APPENDIX 5 (continued)

Experimental results and computer model's

(Example)

CHCl ₃ Flow rate (cc/sec)	Conversion(%) (experiment)	Conversion(%) (computer model)
9.0×10^{-4}	74.93	74.05
2.48×10^{-3}	92.96	81.33
5.63×10^{-3}	92.34	87.12
1.13×10^{-2}	86.31	86.64
2.16×10^{-2}	71.12	77.08
5.09×10^{-2}	38.57	50.47
7.90×10^{-2}	34.82	36.84
8.89×10^{-2}	24.45	33.58

SELECTED BIBLIOGRAPHY

- (1) F.H. Garner , R. long , A.J Graham , and A.Badakshan , Sixth Symposium (International) on Combustion , New York : Reinhold , 1957 , p. 802 .
- (2) W.E Jones , S.D. Macknight , and L. Teng , Chem. Rev., vol. 73 , p. 407 (1973) .
- (3) R.G Gann , ACS Symp. Ser. vol. 16 , 318 (1975) .
- (4) Le Bras, G. , Hajal , I. , Combourieu , J. , and Laffitte , P. : J. Chim, Phys. 64 , 1153 (1967)
- (5) A.A. Westenberg and N. DeHaas , J. Chem. Phys. , vol. 62 , 3321 (1975)
- (6) J.Combourieu , G. Le Bras , and C. paty , Fourteenth Symposium (International) on Combustion , The Combustion Institute , 1973 , p. 485
- (7) W.E Wilson Jr. , J.T. O'Donovan , and R.M. Fristrom , Twelfth Symposium (International) on Combustion , The Combustion Institute , 1969 , p. 929 .
- (8) A.G. Gaydon and H.G Wolfhard , Proc. Royal Soc. London , vol. A 213 , 366 (1952) .
- (9) M. Costes , G. Donthe , and M. Destriaa , Chem. Phys. Lett. , vol. 61 , 588 (1979) .
- (10) S.J. Arnold , G.H. Kimbell , and D.R. Snelling , Can. J. Chem. , vol. 53 , 2419 (1975)
- (11) W.E. Jones , G. Matinopoulos , and J.S. Wasson , J. Chem. Soc. Faraday Trans. II , vol. 73 , 831 (1978) .
- (12) P.L Gould and G.A Oldershaw . Inter. J. Chem Kine. , vol. 14 , 1105 (1982)
- (13) Brice Carnahan , H.A. Luther , and James O , Wilkes . N.Y. Wiley (1969) .
- (14) Rosenbrock , H.H. " An Automatic Method for finding the greatest or least value of a function " Computer J. 3 , 175-184 , 1960 .
- (15) P.N. Clough et. al. , Chem. Phys. Lett., vol. 23 , 155 (1973)
- (16) A. Mckenzie , M.F.R. Mulcahy , and J.R. Steven , J. Chem. Soc. Faraday Trans. I , vol. 70 , 549 (1974)

- (17) R.H Perry and C.H Chilton , Chemical Engineers' Handbook , New York : McGraw-Hill , 1973 .
- (18) O. Levenspiel , Chemical Reaction Engineering , New York : Wiley , 1972 .
- (19) I. Langmuir , Trans. Amer. Electrochem. Soc. , 20 , 225 (1911) .
- (20) Joseph W.Bozzelli and Robert Barat . Rev. Sci. Instrum. 52 (4) , Apr. 1981 .
- (21) F.C. Fehsenfeld , K.M. Evenson , and H.P Broida . Rev. Sci. Instrum. 36 (3) , Mar. 1965 .
- (22) K.R. Jennings and J.W. Linnett , Nature (London) , 182 , 597 (1958) .
- (23) Sriram Chari , " Reactions of Atomic Hydrogen with Selected Halomethanes " , 1981 .
- (24) J.W. Bozzelli and J.Snyder , J. Chem. Educ. , vol. 58 , 522 (1981)
- (25) R.C. Weast , CRC Handbook of Chemistry and Physics , Cleveland: CRC Press , 1977 .
- (26) A.A. Westenberg and N. de Hass , J. Chem. Phys. 48 , 4405 (1968) .
- (27) J.H. Lee , J.V. Michael , W.A. Payne , L.J. Stief , and D.A. Whytock , J. Chem. Soc. Faraday Trans. I 73,1530 (1977)
- (28) R.T. Watson , J. Phys. Chem. Ref. Data 6 , 871 (1977) .
- (29) M.A.A. Clyne and D.H. Stedman , Trans. Faraday Trans. 62, 2164 (1966) .
- (30) P.F. Ambidge , J.N. Bradley , and D.A. Whytock , J. Chem. Soc. Faraday Trans. I 72 , 2143 (1976) .
- (31) J.C. Miller and R.J. Gordon , J. Chem. Phys. 75 (11) , Dec. 1981 .
- (32) M.A.A. Clyne and R.F. Walker J. Chem. Society , Faraday Trans. I , 1547 , vol. 69 (1973) .
- (33) D.T. Clark and J.M. Tedder , Trans. Faraday Soc. , vol. 62 , 393 (1966) .
- (34) B.deB. Darwent , Bond Dissociation Energies in simple Molecules , Washington : National Standard Reference Data System , 1970 .

(35) F. Westley , Table of Recommended Rate Constants for Chemical Reactions occurring in Combustion , Washington : National Standard Reference Data System , 1970 .

(36) (a) Maia Weissman and S.W. Benson , "The Pyrolysis of Methyl Chloride . A Pathway in the Chlorine-catalyzed Polymerization of Methane " . (b) S.W. Benson , "Thermochemical Kinetics " , John Wiley & Sons, New York .

(37) R.F. Jansson , Chem. Commun. 14, 320 (1965) .

(38) D.M. Silver and N. de Hass , J. Chem. Phys. , Vol. 74, 1745 (1981).

(39) T.E. Kleindienst and B.J. Finlayson-pitts, Chem. Phys. Lett., Vol. 61, 300 (1979).